

# CHALMERS



## Tire thermal analysis and modeling

At Renault SA Innovative Chassis Department

Master's Thesis in Automotive Engineering

SÉBASTIEN CHALIGNÉ

Department of Applied Mechanics

*Division of Vehicle Engineering & Autonomous Systems*

CHALMERS UNIVERSITY OF TECHNOLOGY

Göteborg, Sweden 2011

Master's Thesis 2011:02



MASTER'S THESIS 2011:02

# Tire thermal analysis and modeling

At Renault SA Innovative Chassis Department

Master's Thesis in Automotive Engineering

SÉBASTIEN CHALIGNÉ

Department of Applied Mechanics  
*Division of Vehicle Engineering & Autonomous Systems*  
CHALMERS UNIVERSITY OF TECHNOLOGY  
Göteborg, Sweden 2011

Tire thermal analysis and modeling  
At Renault SA Innovative Chassis Department  
Master's Thesis in Automotive Engineering  
SÉBASTIEN CHALIGNÉ

© SÉBASTIEN CHALIGNÉ, 2011

Master's Thesis 2011:02  
ISSN 1652-8557  
Department of Applied Mechanics  
Division of Vehicle Engineering & Autonomous Systems  
Chalmers University of Technology  
SE-412 96 Göteborg  
Sweden  
Telephone: + 46 (0)31-772 1000

Cover: the top picture illustrates a Renault Megane III R.S. cornering with high sideslip angle, which represents a case where the temperature is of paramount importance for tire behavior. The bottom left picture represents a tire positioned on the MTS Flat-Trac during indoor tests and the bottom right picture taken with a thermal camera illustrates the surface temperature of the rotating tire.

Chalmers Reproservice / Department of Applied Mechanics  
Göteborg, Sweden 2011





Tire thermal analysis and modeling  
At Renault SA Innovative Chassis Department  
Master's Thesis in Automotive Engineering  
SÉBASTIEN CHALIGNÉ

Department of Applied Mechanics  
Division of Vehicle Vehicle Engineering & Autonomous *Systems*  
Chalmers University of Technology

## ABSTRACT

Tires are of paramount importance in vehicle dynamics. They are the only vehicle's components in contact with the road and hence transmitting necessary forces and moments for the vehicle to accelerate, brake and turn. So far, temperature influence on tire behavior has not hold car manufacturers' interest so much. Tire models were usually limited to be mathematical models taking into account tire and axle geometry mechanical properties, normal load and inflation pressure. However, some differences appeared when comparing forces and moments estimated by tire models and measured test data. Part of these differences is now believed to be due to variation in tire thermal properties when the tire is subject to different stress types (slip and camber angles, normal load, inflation pressure, vehicle speed...).

The aim of this study is to perform a thermal analysis of the tire. How its surface temperature varies depending on various conditions and how these variations influence the tire behavior will be of prior concern. Hence, some indoor tests will be performed by positioning the tire on the MTS Flat-Trac® III tire test system and using infrared sensors to measure the tire surface temperature. Experiments will be based on an experimental design where all the parameters believed to have an influence on the tire temperature will vary. Results will allow understanding which parameters are of primary importance for the temperature and will also be used to build up an empirical tire thermal effects model. This latter will be used in parallel with the currently used Pacejka model and take into account the variation of tire performance in terms of lateral forces. Eventually, the validation of the model will be done performing full vehicle tests.

Keywords: Tire model, Thermal effects, Temperature influence, Lateral force, Vehicle dynamics, Experimental design





# Contents

ABSTRACT	I
CONTENTS	III
PREFACE/ACKNOWLEDGMENT	V
TABLE OF FIGURES	VI
NOTATIONS	VII
1 INTRODUCTION	1
1.1 Purpose	1
1.2 Limitations	2
1.3 Approach used	2
1.4 Theoretical background	2
1.4.1 Tire review and hysteresis phenomenon	3
1.4.2 Delft-Tyre 96' model	4
2 LITERATURE SURVEY ON TIRE MODELS	7
2.1 TaMeTire model from Michelin	7
2.2 T3M from Tüv Süd Automotive	8
2.3 Toyota tire lateral force model	10
2.4 Summary	11
3 MATERIALS	13
3.1 MTS Flat-Trac III CT	13
3.2 Infrared temperature sensors	14
3.3 Full-vehicle equipment	16
4 SENSITIVITY STUDY	17
4.1 Design of experiment	17
4.2 Parameters influence on tire temperature	19
4.3 Temperature influence on tire transversal behavior	21
4.3.1 According to the literature	21
4.3.2 Flat-Trac experiments	22
5 TIRE THERMAL MODEL DEVELOPMENT	25
5.1 Tire tread temperature model	25
5.1.1 Physical temperature model	25
5.1.2 Empirical temperature model	26
5.1.3 Coefficients optimization	27

5.2	Lateral force model with thermal effect	29
5.2.1	Model construction	29
5.2.2	Coefficients optimization	30
6	EXTENSION OF THE MODEL TO VEHICLE USE	34
6.1	Ambient temperature and aerodynamics influences	34
6.2	Temperature modeling	35
6.3	Conclusion	38
7	CONCLUSION	40
	APPENDICES	42
	Appendix A: Delft-Tyre model details in x and y directions	42
	<i>Steady-state longitudinal direction (pure slip)</i>	42
	<i>Steady-state lateral direction (pure sideslip)</i>	43
	Appendix B: Infrared temperature sensors specifications	44
	Appendix C: Test matrix from the experimental design	45

## **Preface/Acknowledgment**

In this study, indoor experiments on a Flat-Trac tire test system and outdoor full vehicle tests have been performed to analyse and model the tire tread temperature and its effects on tire transversal behaviour. These tests have been carried out from January to July 2010. The work is a part of a Renault research project concerning tire properties and named ATLAS 2. The project is carried out at the Innovative Chassis Department of the Renault Test Center in Aubevoye, France.

This part of the project has been carried out with Julien COMTE (tire research engineer at Renault SA) as supervisor. Indoor tests have been carried out with Frédéric HAMON and Pascal BLANC (Flat-Trac technicians at Renault SA) and their help with measurement devices and building test profiles has been highly appreciated. Full vehicle tests have been prepared and performed with the help of Bruno DUPUIS (Chassis validation specialist at Renault SA). Finally, I would like to thank Mathias LIDBERG (researcher/teacher at the Applied Mechanics department of Chalmers University) as my Chalmers instructor for permitting me to do this interesting thesis in the vehicle dynamics field and for his involvement during the thesis.

Aubevoye (FRANCE), July 2010

Sébastien Chaligné

## Table of figures

FIGURE 1: SCHEMA OF A POSSIBLE IMPLEMENTATION OF A THERMAL EFFECT MODEL.....	1
FIGURE 2: TIRE GENERAL STRUCTURE.....	3
FIGURE 3: TIRE RUBBER OPERATING DOMAIN [9].....	4
FIGURE 4: COMPARISON OF $F_Y$ FROM DELFT-TYRE MODEL AND MEASUREMENTS.....	5
FIGURE 5: MICHELIN TAMETIRE MODEL - INPUTS AND OUTPUTS.....	7
FIGURE 6: MICHELIN TAMETIRE MODEL - HEAT EXCHANGES.....	8
FIGURE 7: MICHELIN TAMETIRE MODEL - LATERAL FORCES MEASURED AND MODELED.....	8
FIGURE 8: T3M - SIMULINK MODEL.....	9
FIGURE 9: T3M - EXAMPLE OF TEMPERATURE RESULTS (X AXIS = TIME AND Y AXIS =TEMPERATURE).....	10
FIGURE 10: TOYOTA MODEL - $F_Y$ AND $T$ MEASURED.....	11
FIGURE 11: TOYOTA MODEL - $F_Y$ AND $T$ MODELED.....	11
FIGURE 12: MTS FLAT-TRAC AT THE RENAULT TEST CENTER OF AUBEVOYE.....	13
FIGURE 13: INFRARED SENSOR CALIBRATION CURVES.....	15
FIGURE 14: STUDIED SYSTEM (TIRE) DEFINITION.....	17
FIGURE 15: SLIP AND CAMBER ANGLES PROFILES (MEASUREMENT SYSTEM VALIDATION).....	18
FIGURE 16: TEMPERATURE RESULTS FOR ALL CONDITIONS OF THE EXPERIMENTAL DESIGN.....	19
FIGURE 17: DIAGRAM OF EFFECTS ON TEMPERATURE IN PURE TRANSVERSAL DIRECTION.....	20
FIGURE 18: MAXIMUM LATERAL FORCE $F_Y$ VERSUS TIRE TEMPERATURE [6].....	21
FIGURE 19: TIRE CORNERING STIFFNESS VERSUS TEMPERATURE [6].....	22
FIGURE 20: $F_Y$ AND TEMPERATURE RESULTS AT 110 KM/H.....	22
FIGURE 21: LATERAL FORCE VARIATION IN FUNCTION OF TEMPERATURE.....	23
FIGURE 22: CORNERING STIFFNESS VARIATION IN FUNCTION OF THE TEMPERATURE.....	23
FIGURE 23: SCHEME OF THE STUDIED TIRE (HEAT BALANCE).....	25
FIGURE 24: EXAMPLE OF PHYSICAL TEMPERATURE MODEL RESULT.....	26
FIGURE 25: TIRE TEMPERATURE MODEL RESULTS.....	27
FIGURE 26: TEMPERATURE MODEL RESULTS (ZOOM IN STATIC AND TRANSIENT CONDITIONS).....	28
FIGURE 27: TEMPERATURE MODEL RESULTS (ZOOM IN NON LINEAR REGION).....	28
FIGURE 28: TIRE TEMPERATURE FOR A SA SWEEP.....	30
FIGURE 29: COMPARISON MODELS FOR SA SWEEP ( $F_Y$ VS TIME).....	31
FIGURE 30: COMPARISON MODELS FOR SA SWEEP (INSTANTANEOUS ERRORS).....	31
FIGURE 31: COMPARISON MODELS FOR SA SWEEP ( $F_Y$ VS SA).....	32
FIGURE 32: AMBIENT TEMPERATURE INFLUENCE (STATIC TEST).....	34
FIGURE 33: ZOOM IN STATIC TEST.....	35
FIGURE 34: TEMPERATURE MODEL ON TRACKS (OPTIMIZATION).....	36
FIGURE 35: TEMPERATURE MODEL ON TRACKS (VALIDATION).....	36
FIGURE 36: LATERAL FORCE MODEL (2 LAPS OF BEHAVIOR TRAK).....	37
FIGURE 37: ZOOM IN OF LATERAL FORCE MODEL (2 LAPS OF BEHAVIOR TRACK).....	37
FIGURE 38: PURE BRAKING/TRACTION CONDITION.....	42
FIGURE 39: PURE CORNERING CONDITION.....	43
FIGURE 40: SLIP AND CAMBER ANGLES FROM THE EXPERIMENTAL DESIGN.....	46

# Notations

## Roman upper case letters

$A_{cp}$	Contact patch area
$A_{total}$	Total tread area along the tire circumference
$C_{\alpha}$	Tire cornering stiffness
$C_Y$	Pacejka shape factor in pure transversal
$D_Y$	Pacejka peak factor in pure transversal
$E_P$	Mean effect of a given parameter
$E_Y$	Pacejka curvature factor in pure transversal
$K_Y$	Pacejka slip stiffness factor in pure transversal
$F_x$	Longitudinal (propulsive) force
$F_y$	Lateral (side) force
$F_z$	Vertical (normal) load
$M_z$	Self-aligning torque
$P$	Tire inflation pressure
$S_x$	Longitudinal slip
$S_{Hy}$	Pacejka horizontal shift at the origin in pure transversal
$S_{Vy}$	Pacejka vertical shift at the origin in pure transversal
$T$	Tire tread temperature
$T_a$	Ambient temperature
$T_m$	Averaged tire tread temperature on a single sideslip stage
$T_{pi}$	Temperature measured for a given parameter (experimental design)
$V$	Vehicle speed
$W$	Heat capacity

## Roman lower case letters

$t$	Time
$c_p$	Specific heat capacity at constant pressure
$q$	Heat flux

## Greek lower case letters

$\alpha$	Slip angle
$\delta$	Steering angle
$\gamma$	Camber angle
$\lambda_t$	Tire rubber thermal conductivity
$\mu$	Tire/road grip – friction coefficient
$\rho_a$	Air density
$\rho_t$	Tire rubber density
$\omega$	Wheel rotational speed



# 1 Introduction

Due to the increasing use of safety systems such as ESP and ABS and the need to develop optimized strategies for these systems, it becomes very important for a car manufacturer to be able to estimate the forces and moments a tire transmits to the road with as much accuracy as possible. Therefore, developing a tire model that can simulate these forces and moments as function of the solicitations the tire is going through and its characteristics is of primary importance. However, currently used models have shown a certain lack of accuracy in some specific cases. This lack of accuracy is believed to be partly due to thermal effects. Actually, the tire tread temperature is not constant on normal operating conditions and this latter induces some changes in tire performance.

## 1.1 Purpose

The purpose of this project can be divided into two parts. The first part consists of getting an understanding on how the tire tread temperature varies with the solicitations it is going through and how this temperature affects its performances in terms of transmissible lateral force. The objective of this step is to quantify the influence of each input parameters (slip angle, vehicle speed...) on the tire temperature and the force changes corresponding to a given temperature variation. The second part consists of modeling the thermal effects observed in the first part.

The tire model used in this study being the Delft Tyre 96'[10] based on the Pacejka magic formula, a final result for this project would be to develop a thermal effect model consisting of a tire tread temperature model and a model of lateral force variations due to the temperature. A possible implementation of such a thermal effect model is illustrated below (grey blocks).

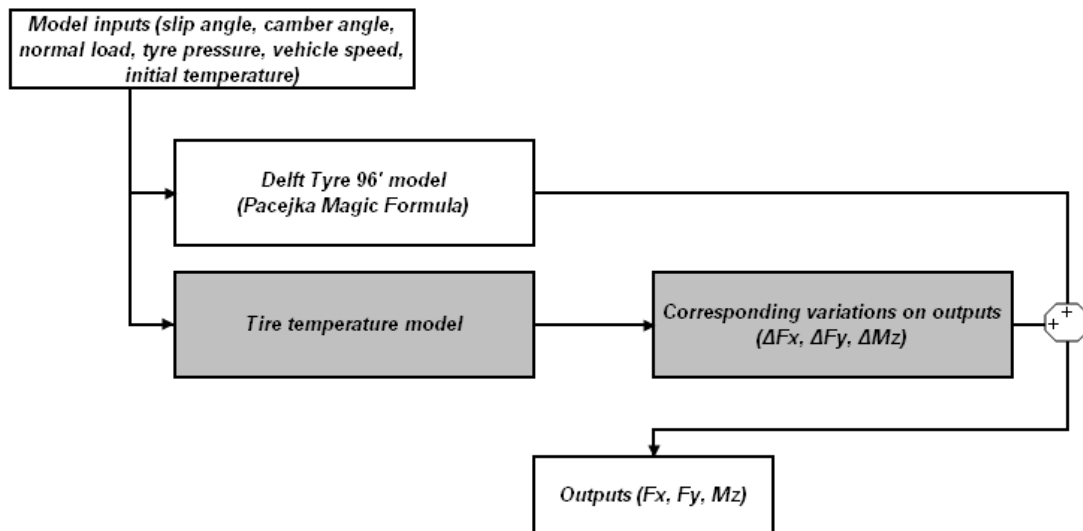


*Figure 1: Schema of a possible implementation of a thermal effect model*

It has to be noted that the model represented in Fig. 1 is a long term objective. Within the scope of this study, the outputs taking into account the thermal effects are only the lateral tire force.

## **1.2 Limitations**

The main limitation of this study is that the Pacejka model is considered as accurate only in steady-state and not in transient conditions. Hence, when experimenting on tires in order to get an understanding on thermal effects, one has to pay attention to keep the tire in steady-state operating conditions so that no discrepancy due to transient conditions interacts. In this way, the variance observed between measured force curves and modeled force curves will be entirely due to temperature effects.

A second important limitation is to conduct experiments in indoor. Actually, when studying tire thermal properties, it is of prior importance for the tire to be in its usual operating environment. For instance, when the tire is rotating on the Flat-Trac roadway, there is no aerodynamic drag coming from the vehicle speed and no wheelhouse to cover it. Hence, the surrounding environment is different and can play a role in the tire surface temperature. In order to check if this affects the tire thermal properties in a non negligible way, the final validation of the model will be done using full vehicle experiments on road conditions.

## **1.3 Approach used**

In order to understand how temperature and forces vary depending on operating conditions, a design of experiment was built. Once this latter completed and test profiles built, a single tire was positioned on an indoor tire test system to be tested. Since this measurement bench named Flat-Trac is generally used to measure forces and moments only, some infrared sensors measuring the tire tread temperature on the top along the tire width were added.

Once all the data needed is obtained, the tire temperature and forces were simulated using Matlab/Simulink. A sensitivity study was performed to determine the influence of each input parameter on temperature as well that of temperature on tire performance. Then it was possible to develop a thermal effects model. Some unknown model parameters, such as friction coefficient variations with temperature were determined experimentally using indoor test on Flat-Trac.

The final model validation has been done using full vehicle experiments on Renault testing tracks. This final step allowed checking if the model was accurate in the real tire surroundings.

## **1.4 Theoretical background**

This part proposes a short review of the theory to be known in order to fully understand the following study. In a first part, the tire and its basic characteristics and properties will be described along with the hysteresis phenomenon. In a second part, the Delft-Tyre model will be explained.



### 1.4.1 Tire review and hysteresis phenomenon

The tire is one of the most essential elements in the automotive field. It plays a preponderant role in car handling performance, road holding and driving comfort. Excluding the aerodynamic drag force, every resistance forces come by the tire road contact patch area. It is also via the tire that the vehicle can accelerate, decelerate or turn. Actually, the tire transmits longitudinal and lateral forces coming from the engine to the road. Furthermore, it has also to withstand the normal load and to assure a first damping of the vibrations coming from the road to maintain a certain comfort for vehicle occupants.

A tire is a very complex system. As shown by the illustration below, a tire consists of a tread mainly made of rubber, some rigid steel belts that can be positioned in radial or diagonal direction, a carcass made of rubber reinforced by glass fiber, nylon and polyester. Bead allows the tire to be fitted into the rim, not represented here.

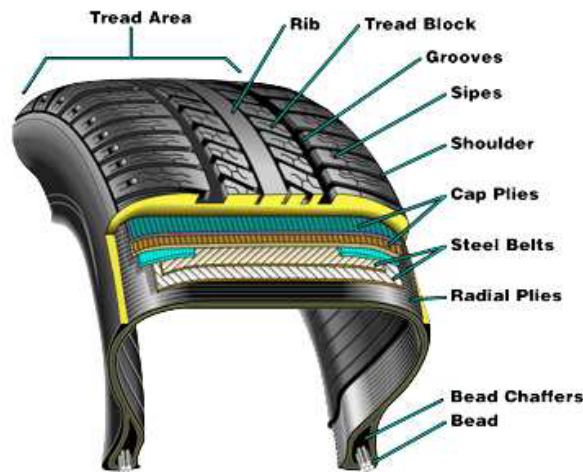


*Figure 2: Tire general structure*

The tread area is the part in contact with the ground when being at its bottom position. Grooves allow draining the water in rain conditions. The carcass withstands the normal load coming from the sprung mass of the vehicle.

As it can be seen in Fig.2, the dominant material used in tire constitution is the rubber, an elastomeric material which the tire gets its adherence capacity from. The rubber is a visco-elastic material, in other words a deformable material with an intermediary behavior between liquid and elastic.

This kind of material can generally be modeled by a spring damper system. Actually, when a compression-traction force is applied on such material as in tire rolling conditions, the compression and then the return to the initial position occur with a certain delay. This phenomenon is known as the hysteresis and consists in a partial energy dissipation of the applied force. This hysteresis phenomenon combined with other rubber properties make the tire a non linear and very complicated system to model by mathematical equations.

The tire behavior also strongly depends on operating conditions such as vehicle speed, inflation pressure and normal load as well as road surface conditions. Two physical parameters very influent on tire rubber behavior are the cyclic frequency (here

proportional to the rotational speed of the wheel) and the rubber temperature, main interest of this study.

At very low temperature, the rubber modulus (defined as the ratio stress/strain) is high. The rubber has a rigid and brittle behavior like glass. On the other hand, at high temperature, the modulus is low. In this case, the rubber is elastic and flexible, it is a rubbery behavior. It is within an intermediary temperature range that the rubber is the most viscous, around a temperature named vitreous transition temperature. In this area, polymer chains are deformable enough so that the chain segments can move. During these motions, these segments scrape together and against their surrounding environment. This friction phenomenon produces a chain segment motion delay (hysteresis). Thus, the rubber has a visco-elastic behavior. In this case, the hysteresis losses reach a maximum as illustrated in Fig.3 [9]. Within this temperature domain, the rubber used in tires operates in normal road conditions. In fact, its flexibility and viscosity are the two key factors for a good adherence between the tire and the road. In other words, the more hysteresis, the higher the tire road grip.

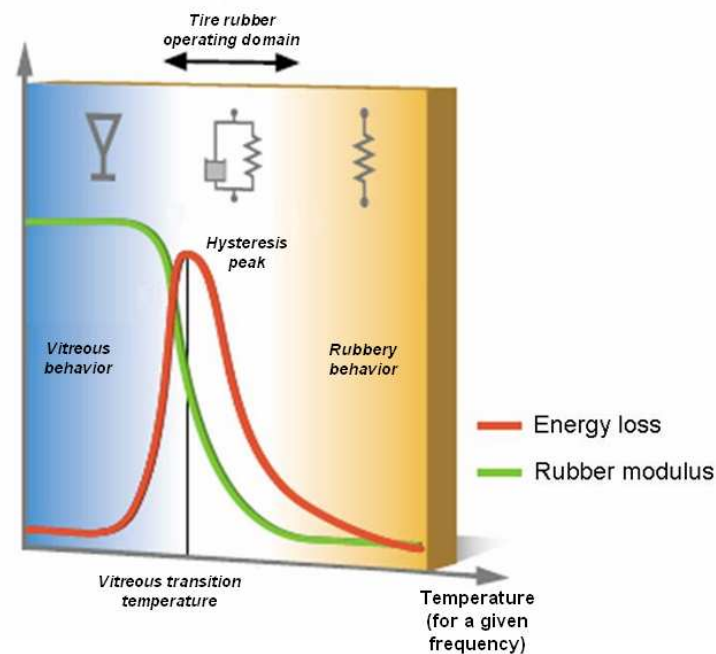


**Figure 3: Tire rubber operating domain [9]**

However, it has to be noted that the previous curves are valid only for a given frequency. Actually, the vitreous transition temperature increases with the frequency. Therefore, the hysteresis peak occurs for a higher temperature when the vehicle speed increases. Theoretically, the energy loss due to the hysteresis is entirely dissipated by heat production. Hence it is easy to understand that this phenomenon should produce non negligible variations in tire tread temperature and therefore changes in tire performance.

## 1.4.2 Delft-Tyre 96' model

For a given tire and road conditions, tire forces and moments due to slip can be estimated by a mathematical formula from the Dr. Pacejka named Magic Formula. The Delft-Tyre 1996 [10] is an empirical tire model based on this formula written

below for pure lateral solicitations. Details of the magic formula in steady-state conditions in pure longitudinal and transversal directions can be found in Appendix 8.1.

$$F_y = F_{y0}(\alpha, \gamma, Fz)$$

$$F_{y0} = D_Y \times \sin^{-1} \times (C_y \times \tan^{-1}(B_y \times \alpha - E_y \times (B_y \times \alpha - \tan^{-1}(B_y \times \alpha)))) + S_{vy} \quad (1.1)$$

$$\alpha = \alpha^* + S_{hy}$$

As it can be seen from the formula above, the Magic Formula is an empirical model partly based on physical parameters.  $\alpha$  and  $\gamma$  are the slip and the camber angles and  $Fz$  the normal load.  $B_y$ ,  $C_y$ ,  $D_y$  and  $E_y$  are Pacejka coefficients identified experimentally and  $S_{hy}$  and  $S_{vy}$  are respectively the horizontal and vertical shift at the origin.

Furthermore, in order to simulate the transient behaviour of the tire, a first order lag of tire longitudinal and lateral deformations are introduced through two relaxation lengths.

An example is shown in Fig 4. where a slip angle sweep (completed in 40 seconds) has been performed on the MTS Flat-Trac tire test system. This allows the reader to get an understanding on curve shapes that can be obtained using this magic formula.

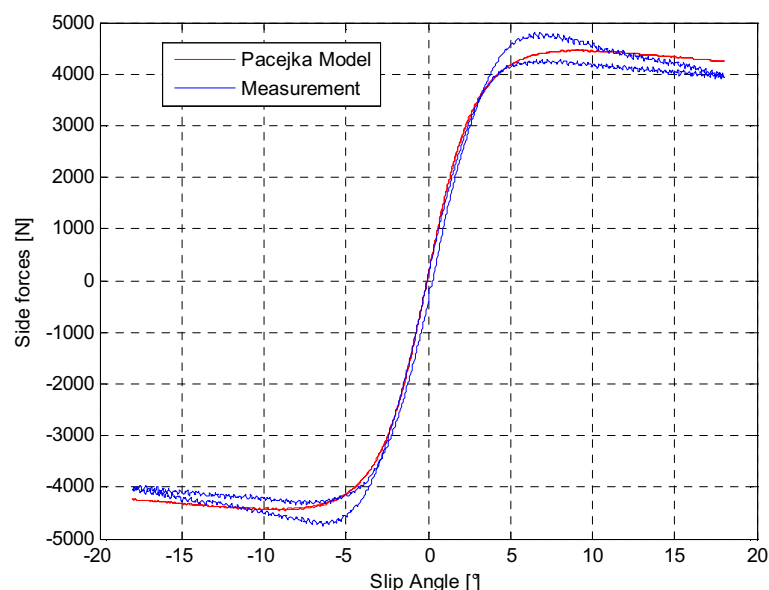


**Figure 4: Comparison of  $F_y$  from Delft-Tyre model and measurements**

Fig.4 shows that the Delft-Tyre model is accurate but could be better in two areas. Actually, in the non linear domain for high slip angles, the model does not take into account the lateral force loss occurring in the slip angle descending phase. It simply estimates the average lateral force of the ascending and descending phase. It can already be said that there must be some room for accuracy improvement in the non linear domain by implementing a thermal effects model. It will be seen later on in this study that this loss is due to an increase in tire tread temperature. Moreover, as said in the limitations part, the transient behavior model could be improved. Actually, in the linear domain, the model does not take into account the occurring delay in a proper way.



## 2 Literature survey on tire models

Several models used to model tire behavior exist and are very well-known by people working in the field of vehicle dynamics. These models such as the brush model or the TM-easy model are also taught in specialized universities. It has to be noted that these models are usually empirical and not physical models. Hence, they have numerous limitations. For instance, they omit to take into account certain physical parameter such as tire tread temperature even if its influence is far from being negligible. Therefore, it would be useless to this study to explain them further.

Very few tire models taking into account thermal effects are available in the literature due to their confidential nature. Actually, car manufacturers and tire suppliers do not communicate so much about their findings. Nevertheless, information on six tire models called “thermo-mechanical” has been found. These models are named that way because they take into consideration the mechanical and thermal behaviors of the tire. This literature survey gathers information about three tire models and on how thermal effects impact on tire performance and how this can be modeled using different means.

### 2.1 TaMeTire model from Michelin

In 2007, Michelin Technologies wrote a patent protecting its TaMeTire (Thermal & Mechanical Tire) model [4][5]. This model allows the tire forces and moments to be estimated in real time for any type of vehicle maneuvers. Lateral force and self-aligning moment are modeled with an impressively high precision for a huge range of sideslip angles and in all cases of tire inflation pressure, speed, normal load and camber angle a tire can be subject to. Furthermore, tire temperature and forces are completely coupled. The main inputs and outputs of this TaMeTire model are illustrated in the figure below.

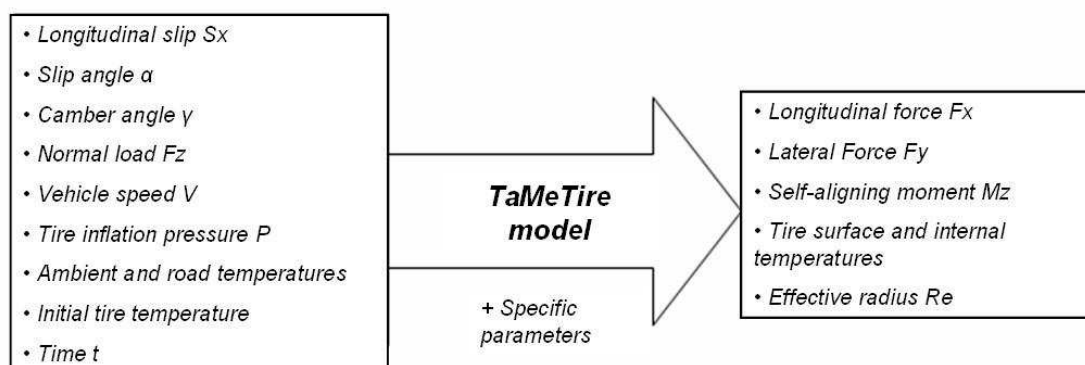


Figure 5: Michelin TaMeTire model - Inputs and outputs [4]

This model consists of three different interacting sub-models: a mechanical model, a local thermal model estimating the tire/road grip variation in function of the tire temperature  $\mu(T)$  and a global thermal model predicting the shear module  $\tau(T)$  still in function of the tire temperature. Only the two thermal models, main interest of this study, will be dealt with in the following.

Radiation exchange phenomena being neglected, they are based on three heat exchange phenomena illustrated as follows depending on tire exchange areas:

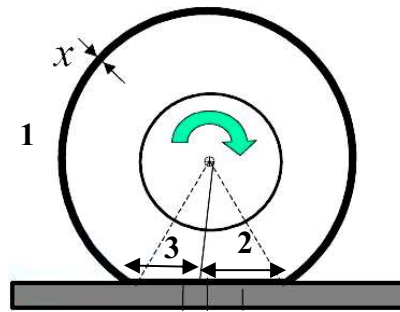


Figure 6: Michelin TaMeTire model - Heat exchanges [5]

Where region 1 is dominated by forced convection to the surrounding air, region 2 by conduction to the track (adherent part) and region 3 by conduction due to friction (sliding part). The tire internal temperature is calculated from the tread surface temperature using the first principle of thermodynamics [4] and can be written as follows:

$$\frac{\partial T}{\partial t} = \frac{\lambda}{\rho_t \times c_p} \times \frac{\partial^2 T}{\partial x^2} + \frac{\dot{q}}{\rho_t \times c_p} \quad (2.1)$$

This way of modelling the tread temperature along with a complicated mechanical model allows predicting the lateral force with an excellent accuracy as it can be seen on the following graph. The orange arrow shows the influence of the normal load  $F_z$  and the blue one emphasizes the influence of the tire tread temperature. In fact, one can observe in the decreasing slip angle phase a drop of lateral force compared to the increasing phase. This is due to the temperature increase in high slip angle cases.

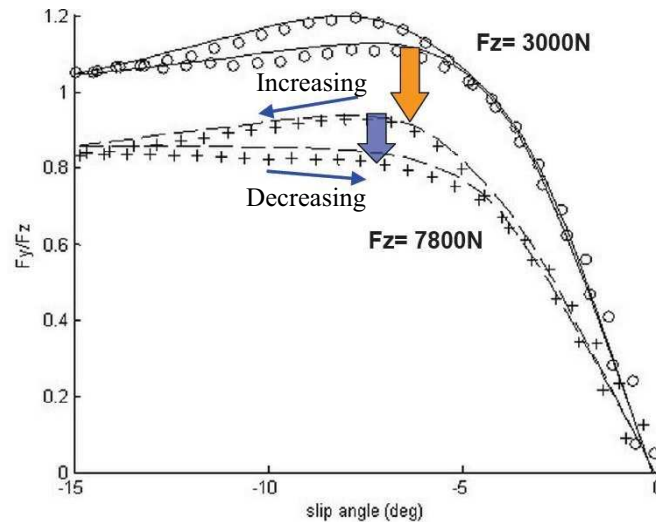
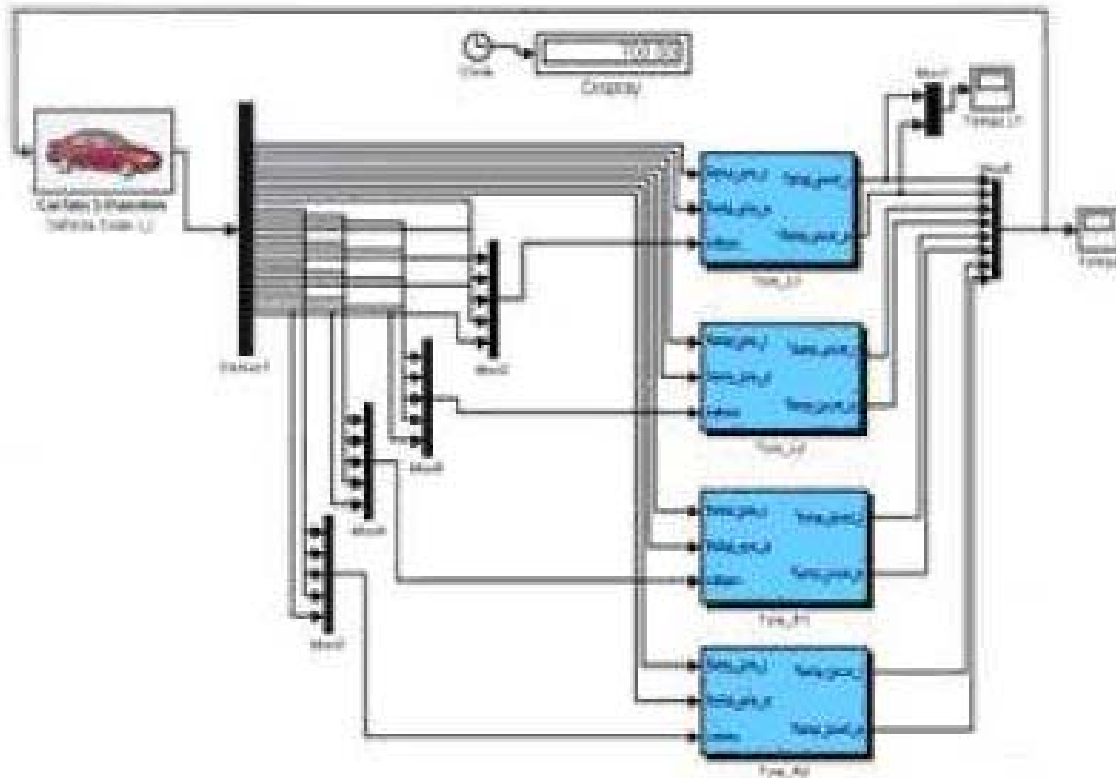


Figure 7: Michelin TaMeTire model - Lateral forces measured and modeled [4]

## 2.2 T3M from Tüv Süd Automotive

Tüv Süd Automotive is a technical consultant and an independent partner in the research and development field for the automotive industry. In the United States in

2005, after the explosion of a few tires causing fatal car accidents, they developed a tire model taking into account the temperature and named *T3M Dynamic Tire Temperature Simulation*. This model is used in series with CarSim and is implemented in Matlab/Simulink. CarSim is an advanced software developed by Mechanical Simulation Corporation that simulates the dynamic behaviour of passenger cars and road conditions. Hence, it includes a tire model. As it can be seen on the Simulink picture below, a temperature model for each tire is linked to a CarSim block and the output temperature goes back to the tire model in CarSim as an input to be taken into account.



**Figure 8:** *T3M - Simulink model [6]*

This model estimating the tire tread temperature is included into each blue block on Fig. 8, each one representing a tire. After going into this temperature model in depth, 6 input parameters have been identified.

- Tire tread temperature a time step earlier
- Normal load  $F_z$
- Slip angle  $\alpha$
- Camber angle  $\gamma$
- Vehicle speed  $V$
- Longitudinal slip  $S_x$

The following graph shows the tire surface temperature during a five minute test. The variance between the measured and the estimated temperatures is very low and never goes up to  $4^\circ\text{C}$  even for very high tire temperatures.

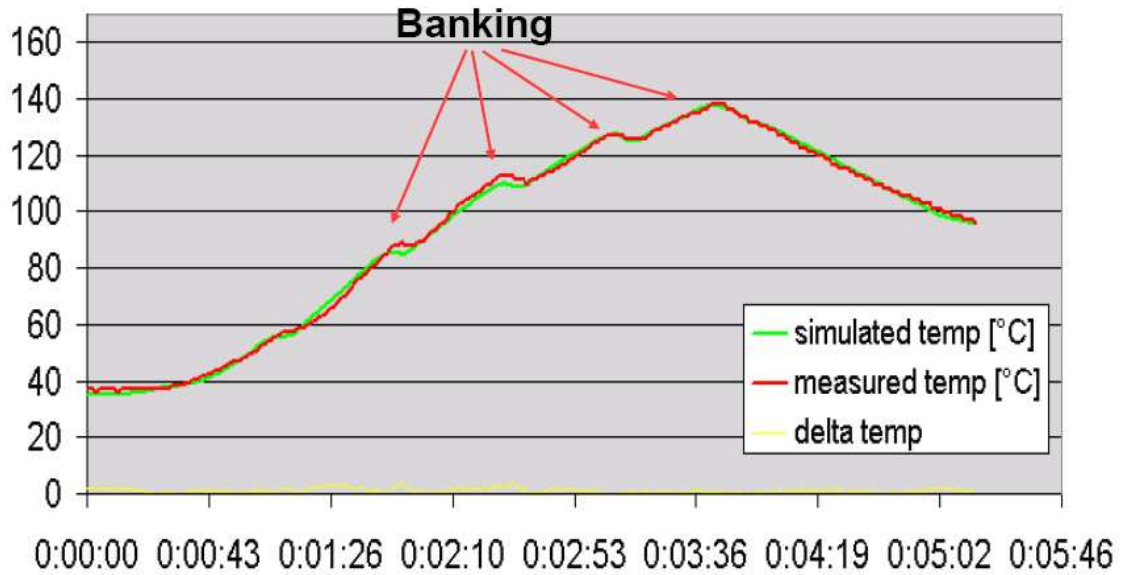


Figure 9: T3M - Example of temperature results (X axis = time (h:m:s) and Y axis =temperature (°C))[6]

### 2.3 Toyota tire lateral force model

The Toyota model [8] is based on the Pacejka's magic formula. In contrary to the TaMeTire model, it estimates only the tire lateral forces  $F_y$  in taking into account the tire surface temperature. The thermal model used here is based on two assumptions that allow doing an energy balance at the tire contact patch. Actually in this paper, they state that heat exchanges within the studied tire are located in the exact same contact patch point and take place at the same time. Considering this and that the heat flux  $q$  is equal to the energy flux due to the tire action on the road, the energy balance in a specific contact patch point can be written as follows.

$$W \times \frac{dT}{dt} = q - \lambda_t \times A_{cp} \times (T - T_a) = F_y \times V \times \alpha - \lambda_t \times A_{cp} \times (T - T_a) \quad (2.2)$$

This equation gives a relationship between the tire tread temperature  $T$  and the lateral force  $F_y$ . It has to be noted that the heat capacity  $W$  and the thermal conductivity  $\lambda$  are determined experimentally.  $T_a$ ,  $A_{cp}$ ,  $V$  and  $\alpha$  are respectively the ambient temperature, the contact patch area, the vehicle speed and the slip angle. Then, as explained earlier, the magic formula is used to determine the lateral force  $F_y$ . However, it can be seen that the Pacejka coefficients used are not constant but function of the tire temperature  $T$ .

By performing a slip angle sweep from  $-20$  to  $20^\circ$  with two different speeds (in order to check transient properties of the model with 4 and 40 second manoeuvres), the lateral force and temperature curves obtained by measuring and by the model can be plotted in function of the slip angle as below and compared.



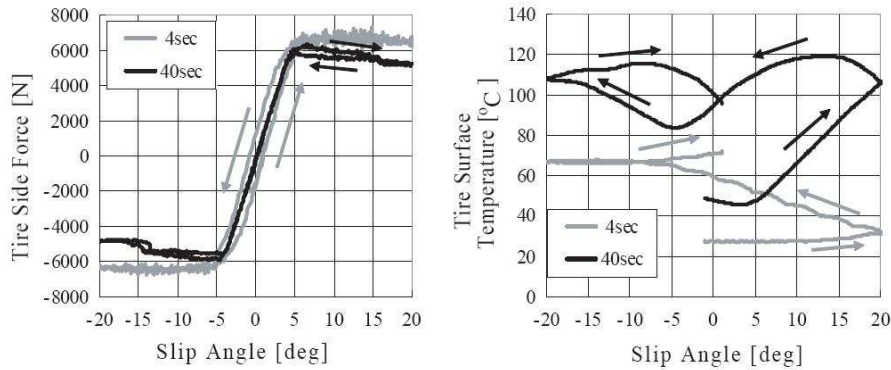


**Figure 10: Toyota model -  $F_y$  and  $T$  measured**

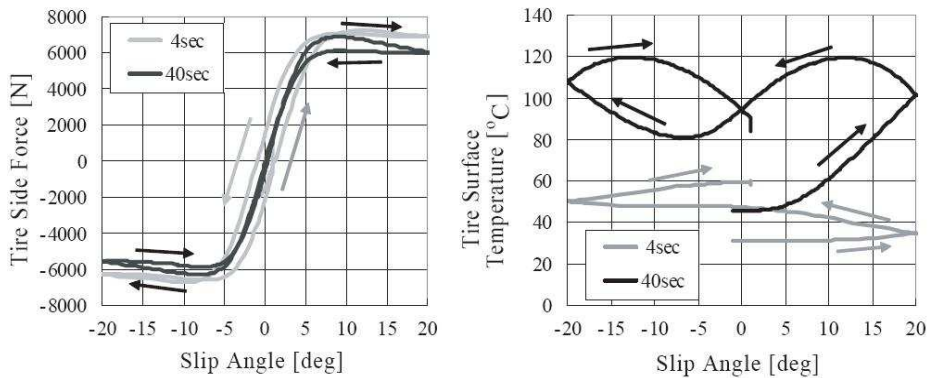


**Figure 11: Toyota model -  $F_y$  and  $T$  modeled**

By comparing the lateral force graphs above, it can be observed that the model predicts the force accurately. Regarding the temperature model, its accuracy seems to be relatively lower but it remains very satisfying considering the studied system, the tire. Another thing that can be seen is that for the slip angle sweep of 4 seconds, the transient conditions imposed to the tire create an important delay and the lateral force is not equal to zero when the slip angle returns to zero. In that case, hysteric phenomena are important and the rubber cannot return to its initial position in such short time.

## 2.4 Summary

As a conclusion of this literature survey, it can be said that there are several ways to model how the tire behaves with a variation of its temperature. Actually, some physical and empirical based models have been investigated. Moreover, the influence of the tire tread temperature on the tire behavior has been emphasized and one can already say that its role is preponderant in the non linear domain (high sideslip). For instance, the TaMeTire model analysis has shown that the temperature cannot be neglected in the non linear region by comparing it with normal load effect (Fig. 7 [4] [5]).



### 3 Materials

In this study, two different test approaches will be used. Actually, in a first step, indoor experiments will be performed in order to get a basic understanding of how the tire temperature varies with the solicitations the tire is going through and what corresponding changes occur in tire performance in terms of the ability to generate lateral force. These indoor experiments will be conducted on a tire test system and will also be used in the model development phase. Then, as a second step of this study, the validation of the developed model will be done using outdoor full vehicle tests.

This part describes the measuring devices and testing machines that are used as well as protocols followed during experiments.

#### 3.1 MTS Flat-Trac III CT

The experiments on tires that have been conducted during the first part of this study were done indoor using a test bench named Flat-Trac. The MTS Flat-Trac III CT (Cornering and Traction) tire test system is designed to perform force and moment testing of passenger car and light truck tires for the acquisition of cornering force data for vehicle handling models and tire characterization. The Flat-Trac bench is shown in the pictures below. It comprises a robust A-frame tire carriage on a stiff structure, advanced measurement devices and a revolving stainless steel roadway providing a flat surface for tire testing. This flat surface is supposed to simulate a high friction coefficient of around 1.



*Figure 12: MTS Flat-Trac at the Renault test center of Aubevoye*

This machine features an automated control system that allows using a personal computer to configure test profiles and analyze the measured data. Designing needed test profiles is simply done using Excel sheets. Main control parameters are slip and camber angles, roadway speed, normal load, longitudinal slip ratio and tire inflation pressure. These control parameters allow the Flat-Trac to reproduce many kinds of road conditions a tire can go through. More experimental conditions can also be reproduced as for instance a slip angle sweep or a tire radial deflection.

### 3.2 Infrared temperature sensors

A previous thesis project [2] at the Renault chassis department is to develop a means of measuring the tire tread temperature on the MTS Flat-Trac with a high enough accuracy and for a limited cost. Among pyrometers, thermocouple and thermal camera, infrared sensors have been chosen.

Nevertheless, a pre-study has been done with a thermal camera lent by another department but retrieving the data for the post-processing was complicated. Moreover, the surrounding environment was hazardous (rubber projection, smoke...) and it was too risky for the camera lens. Therefore, this measurement system has been abandoned quickly.

The infrared sensors used during this project come from Micro-epsilon Optris [14]; a company specialized in infrared temperature measurement devices. The complete specifications can be found in Appendix 8.2. Another infrared sensor used by Renault was available, the Texys [15] but its specifications are unfortunately unknown.

According to this previous project [2], the maximum temperature difference measured around the tire circumference is not up to 1°C. Obviously, this is not significant regarding sensors accuracy of +/-2°C. When conducting experiments on the Flat-Trac bench, three infrared sensors could be used. Therefore, it has been decided to measure the temperature only at the top along the tire width as on the following picture.



Then, in order to have only one temperature value to study, an average of these three temperatures will be calculated. Why it is possible to do that will be explained further.

An important parameter to pay attention to when positioning the sensors is the focal distance between the tire surface and the sensor lens. In fact, this distance determines the area (point) where the temperature is measured and an optimal value exists for this distance. As it can be observed from the left picture above, sensors from Texys (placed in the centre) and from Optris (outer and inner sides) have different optimal distances. Furthermore, another constraint is that sensors need to be positioned perpendicularly to the measured tire surface.

As every type of sensor, infrared sensors need to be calibrated. This is done using an oven where a piece of tire rubber is placed in. After having programmed the oven to a chosen temperature and the temperature inside becomes constant, the temperature is read using a thermocouple. Then, assuming that the piece of rubber has the same temperature as the surrounding air within the oven, the infrared sensor is positioned to

measure the temperature of the piece of rubber in order to check the tension indicated. Therefore, a relationship between the tension and the rubber temperature is found for one point. This process is to be iterated for several temperatures in order to find a calibration curve. Obtained calibration curves can be found on the graph below.

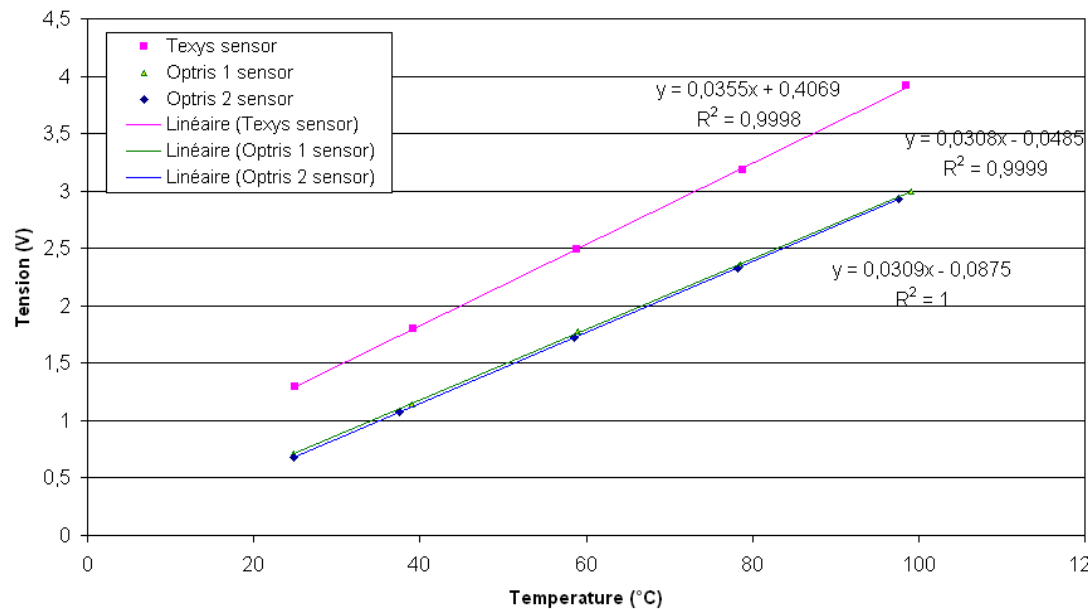


**Figure 13: Infrared sensor calibration curves**

Regarding infrared temperature sensor measurement errors, they are mainly due to three different factors.

- Infrared sensor accuracy with an error of about +/- 2°C on the indicated temperature value.
- Tire tread grooves that slightly modify the focal distance during cornering (especially for high slip angles). Thus, the focal distance is not always optimal.
- Aggressive environment due to dust, smoke and rubber particles that might stay in suspension, reflect light to the sensor lens and hence introduce discrepancies in the measurement data. In order to minimize this phenomenon occurrence, a blowing air nozzle is used to get rid of the rubber particles on the sensor lens.

Other sources of errors are usually systematic and usual for any types of experiments. It has to be noted that the indicated temperature precision is not so high considering the numerous sources of errors. Therefore, the precision objective for the temperature model that will be depicted later has to be set in consequence.

### 3.3 Full-vehicle equipment

In order to validate the thermal effects model on vehicle at the end of this study, some full vehicle tests have been performed on Aubevoye tracks. The same physical parameters of these used on the Flat-Trac bench needed to be measured and therefore, it was necessary to equip a vehicle with proper measurement systems. The test setup will be quickly explained in this part.

The measurement system consists of four devices: two GPS (Global Positioning System) antenna, an IMU (Inertial Measurement Unit), a dynamometric wheel and infra-red sensors. The dynamometric wheel consists of strain gauges measuring forces in the three space directions. The IMU is a combination of accelerometers and gyroscopes measuring orientations, velocities and accelerations in all directions. By combining these three types of device, it is possible to measure every tire model inputs such as slip and camber angles for instance. The slip angle is measured with an accuracy of  $\pm 0.1^\circ$  and does not depend on road irregularities.

The three infra-red sensors measure the tire tread temperature. However, it was not possible to install a nozzle to blow air on the sensor lenses as on the Flat-Trac bench. Therefore, a problem occurs with dust and rubber particles. Hence, the set up is slightly different and uses small mirrors with a 90 degree inclination to prevent this phenomenon from happening. Moreover the wheelhouse is also protected by a brush to prevent gravel projection on sensor lenses.

## 4 Sensitivity study

In this part, a sensitivity study will be performed. This study is aimed to analyze how the tire tread temperature varies with different input parameter variations and how this temperature variation impacts on tire behaviour in terms of transmissible lateral force.

### 4.1 Design of experiment

In order to properly design an experiment, it is of paramount importance to have a good understanding of the studied system. Fig.14 illustrates the studied tire with possible input parameters that one can command on MTS Flat-Trac tire test system and measured output parameters.

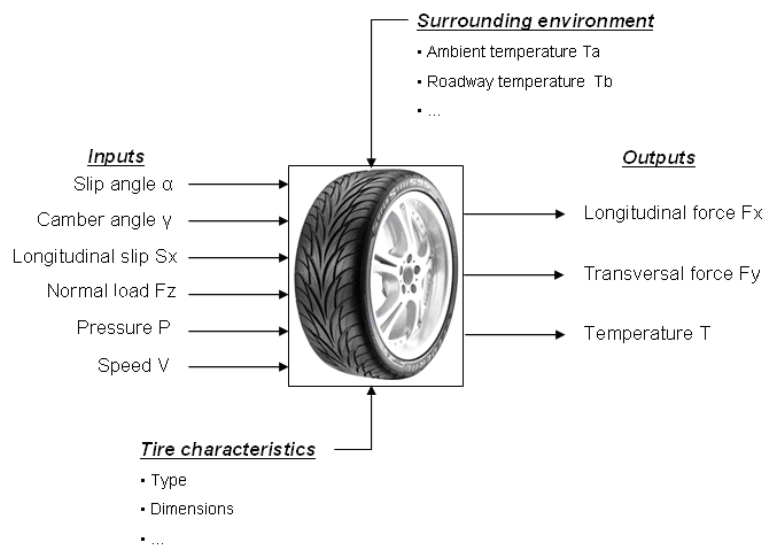


Figure 14: Studied system (tire)

The main purpose of this design of experiment is to understand how the temperature  $T$  is influenced by variations of the input parameters. Therefore, input parameters are changed in a defined way when conducting experiments on Flat-Trac. This way depends on several things as for instance the measurement system performance and which input parameter should be modified more often.

Prior to define the experimental design, a pre-study has been done aimed to validate the choice of averaging the three measured temperatures to get a single tire tread temperature value. In others words, even if this tire temperature measurement technique is used by many, the objective of this pre-study is to validate the test setup defined previously [2]. Hence, a test profile in which temperature variations on both inner and outer tire sides occur was built. It has been decided to perform a test with four different conditions of camber and slip angles ( $\alpha = -/+5^\circ$  and  $\gamma = -/+5^\circ$ ). This test profile is represented in Fig. 15 and allows a strong solicitation of both tire sides and thus checking if the average of the measured temperatures is similar in different cases. Furthermore, this test could also allow reducing the number of tests. Actually, it is possible to check the influence of the slip and camber angle signs which could be negligible. This could be interesting for this study since one could consider only the

absolute value of the angles, thus reducing the total number of experiments conducted.

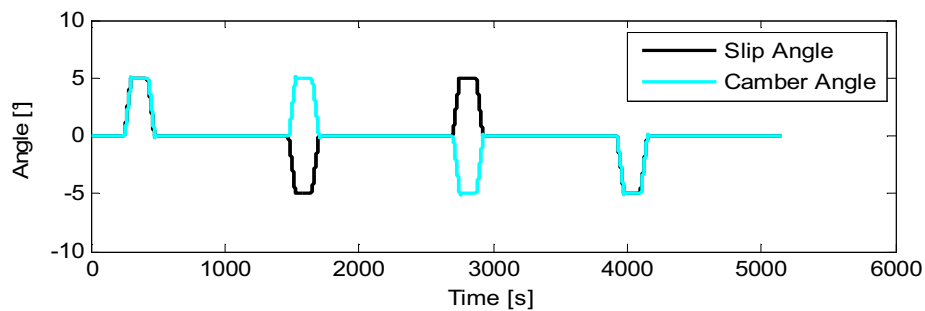


Figure 15: Slip and camber angles profiles (measurement system validation)

When the temperature measured by the three infrared sensors is averaged in each of the four cases, it has been noticed that the temperature in cases 1 and 4 are identical. The same similarity can be observed in cases 2 and 3. The maximum difference is less than two degrees and therefore less than the IR sensor accuracy, which means that this difference is not significant. Therefore, this measurement test setup can be used for the purpose of this study. Moreover, the similarities between cases 1 and 4 and cases 2 and 3 shows that the sign of the camber angle has no effect on the tire tread temperature. For this reason this sign will be neglected in the following (except for the model validation part) and only absolute camber angle values will be used.

The next step is to design the experiment for pure transversal solicitations (the longitudinal slip is controlled and kept to zero). As seen previously, the five input parameters that can affect the tire temperature are the slip angle  $\alpha$ , the camber angle  $\gamma$ , the normal load  $F_z$ , the tire inflation pressure  $P$  and the vehicle speed  $V$ ). The method used is the complete factorial design. The principle of this type of experimental design is to make input parameters vary on two levels: a high level (+) and a low level (-). This allows reducing considerably the total number of experiments to conduct. The following table contains variation domains and chosen levels for each input parameters.

Table 1: Design of experiment (variation domains and levels)

	Variation domain	Low level	High level	Unit
Slip angle $\alpha$	[-18 ; 18]	0	-/+ 5	°
Camber angle $\gamma$	[-5 ; 5]	0	5	°
Speed $V$	[0 ; 150]	30	110	km/h
Normal load $F_z$	[2000 ; 8000]	2500	6000	N
Pressure $P$	[1,8 ; 3,4]	1,8	3,4	bar

These variation domains mark the boundaries of an experimental domain in which linear and/or quadratic dependencies between the tire tread temperature and input parameters exist. To keep this assumption valid, high slip angle level is set to 5° (instead of 18°) to stay in the linear region. Eventually, the design of experiments consists of 32 cases. The most complicated input parameters to change should be modified as less as possible during tests. For instance, the needed time to increase the tire inflation pressure from 1.8 to 3.4 bars is more important than the time needed to vary the camber angle. In the right order, the slip angle will be modified the most frequently, then the camber angle, the normal load, the speed and finally the pressure.



The complete test matrix summing up the experimental design is detailed in Appendix 8.3.

## 4.2 Parameters influence on fire temperature

Experiments were conducted with a single tire, a Continental Contact Premium 2 205/60 R16 96V Extra Load. Once experiments completed, temperature data were post processed to plot tire surface temperature curves for every cases as below.

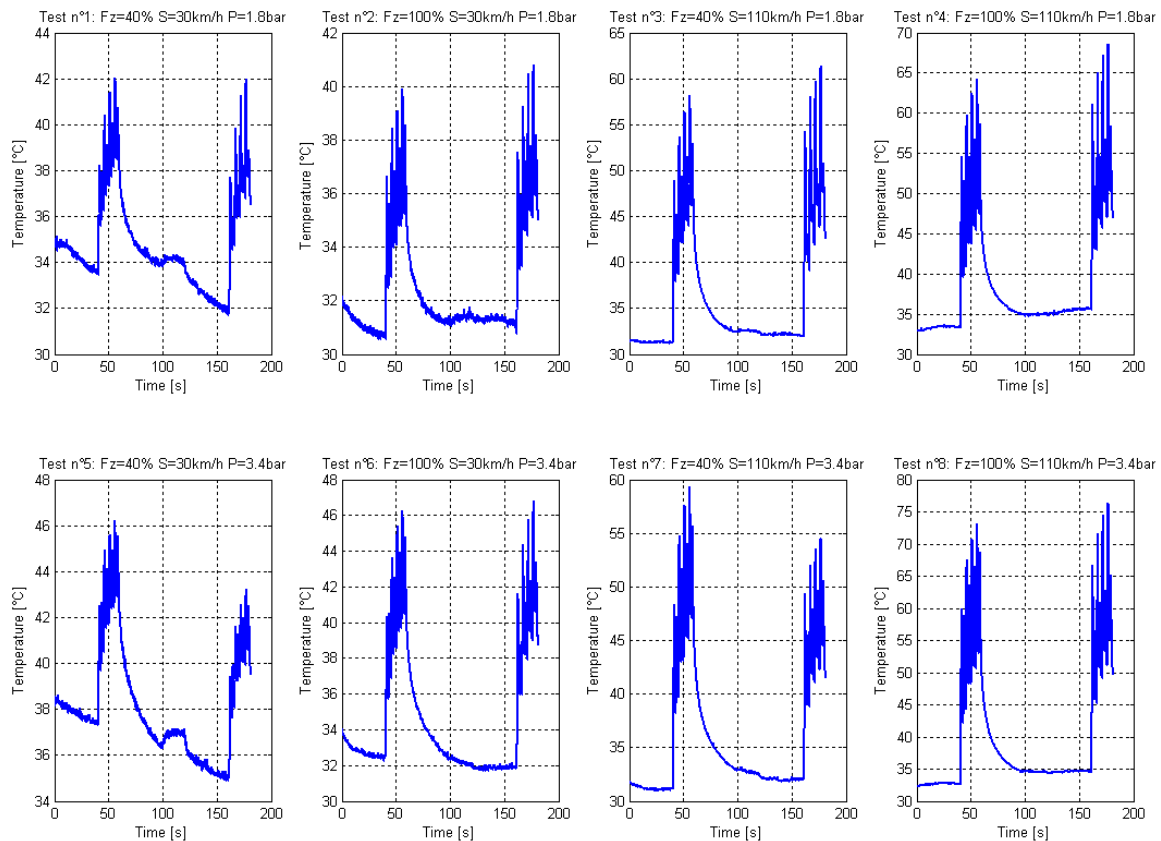


**Figure 16: Temperature results for all conditions of the experimental design**

The following step consists of calculating the influence of input parameters and their interactions on the tire tread temperature. The method used is very simple. For each 32 cases, the measured tire temperature is averaged. Then, for each input parameters and interactions, the formulation below is used to calculate the mean effect of the input parameter  $P_i$  on the temperature.

$$E_P = \frac{\sum_{i+=1}^{i+=16} T_{pi+} - \sum_{i=-1}^{i=-16} T_{pi-}}{\sum p_i} \quad (4.1)$$

where:

- $P$  is an input parameter or interaction between two parameters
- $T_{pi+}$  is the temperature obtained when the parameter  $P$  takes its high level value
- $T_{pi-}$  is the temperature obtained when the parameter  $P$  takes its low level value

- The sum of pi here is equal to the number of cases, 32.

Once the effects calculated, the following histogram can be plotted. It allows to check easily which input parameter is very influent on the temperature and to quantify its effect.

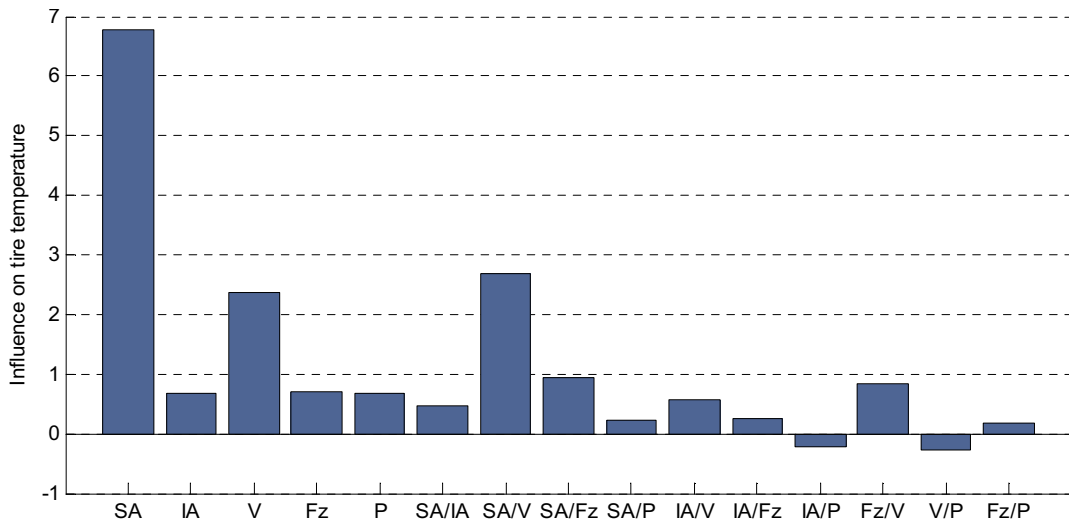


**Figure 17: Diagram of effects on temperature in pure transversal direction**

One can see that the slip angle is by far the input parameter that is the most influent on the tire tread temperature. This is probably due to the sliding phenomena between the tire and the road surface when the slip angle differs from zero. In fact, the more slip angle increases, the more the tread temperature increases.

The second most influent parameter is clearly the vehicle speed. The tricky thing about the speed is that according to the diagram above, it seems that an increase of speed results in an increase in temperature. However, this is true only when cornering ( $\alpha \neq 0$ ). When cornering, the tire tread temperature increases a lot with the speed. This can be seen with the interaction SA/V on the diagram. When rolling in straight line, the vehicle speed has no significant effect on the temperature. It has been seen while testing that an increase in speed makes the temperature slightly decrease due to an increase in cooling phenomena (rotating drag) by forced convection with the surrounding air.

The normal load and inflation pressure are two parameters with a similar influence on the temperature. They are non significant (see Table 2) especially in straight line rolling. However, on Fig.16, it seems that an increase in pressure or normal load increases the temperature while cornering. Regarding the camber angle, its influence is negligible as well. This is due to the fact that when the camber angle is modified, a rise of the outer side temperature occurs but an equal decrease of temperature occurs at the inner side. Therefore, the averaged temperature remains quasi constant. It will be seen later that this phenomena is not of importance when considering the tire behavior.

Table 2 shows which input parameter is significant. To date, the sensor measurement error is about +/- 2°C and the effect error is calculated by  $\Delta E = \frac{\sigma}{\sqrt{n}} = 0.354$  with n=32 here.

*Table 2: Significant effects on temperature*

	<b>Mean effects</b>	<b>Significant effect?</b>
<b>Slip angle</b>	3.39	Significant
<b>Camber angle</b>	0.34	Non Significant
<b>Speed</b>	1.19	Significant
<b>Normal load</b>	0.35	Non Significant
<b>Pressure</b>	0.35	Non Significant

### 4.3 Temperature influence on tire transversal behavior

In this part, the tire tread temperature influence on the lateral force will be studied. In other words, the question “How does the lateral force  $F_y$  vary with the tire temperature?” will be answered. This analysis is divided into two parts. The first part consists of a literature survey and the second of experiments on a tire to study the lateral force variation with the tire temperature.

#### 4.3.1 According to the literature

According to several sources [1][4][5][6][8], the maximum transmissible tire lateral force decreases with a tread temperature increase. It is important to note that for a given normal load (which is the case here), this maximum lateral force is proportional to the tire/road grip. Actually, it is equal to the tire/road grip  $\mu$  times the normal load. Therefore a first conclusion is that the grip is function of the tire temperature which coincides with information found when studying the TaMeTire model from Michelin [5].

The following histogram illustrates how the maximum lateral force decreases with the temperature. This decrease can be quantified to about  $9.5^\circ\text{C}/\text{N}$ .

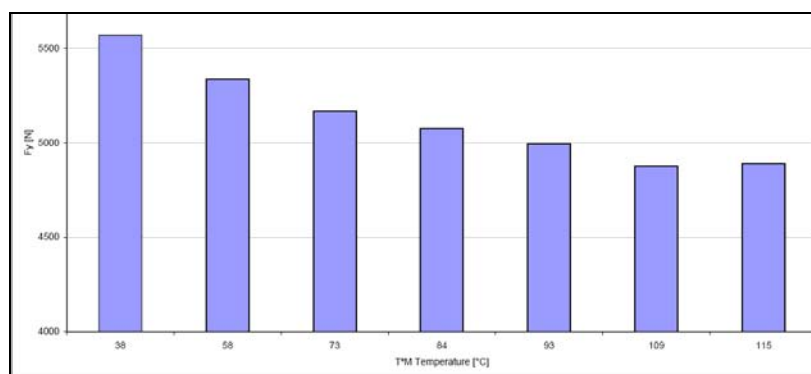


*Figure 18: Maximum lateral force  $F_y$  in Newton versus tire temperature in  $^\circ\text{C}$  [6]*

The second parameter varying with the tread tire temperature is the tire cornering stiffness. Actually, according to Tüv Süd Automotive [6], the cornering stiffness decreases strongly with the temperature (35% of the initial cornering stiffness at ambient temperature with an increase of  $75^\circ\text{C}$  of temperature). The histogram below illustrates this statement.

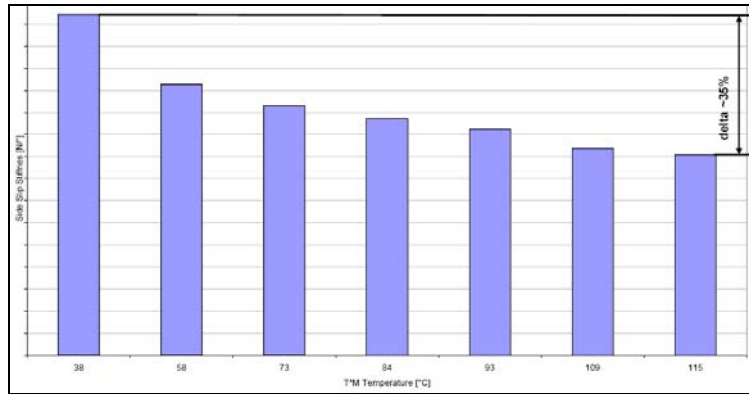


Figure 19: Tire cornering stiffness versus temperature [6]

### 4.3.2 Flat-Trac experiments

In order to check the conclusions from the previous part, some experiments on the Flat-Trac bench has to be conducted. The objective of these experiments is to quantify the maximum lateral force and cornering stiffness variations as function of the tire temperature. To achieve this, the idea is to perform constant slip angle stages in order to increase the tire temperature. Hence, six different slip angle stages have been performed by the tire for two different speeds. The camber angle is kept to zero and the normal load and the inflation pressure remain constant during sideslip stages. These choices of test profiles have been made considering the temperature sensitivity study results in the transversal direction. The figure below illustrates the measurements performed for the 8 degree sideslip stage at 110 km/h.

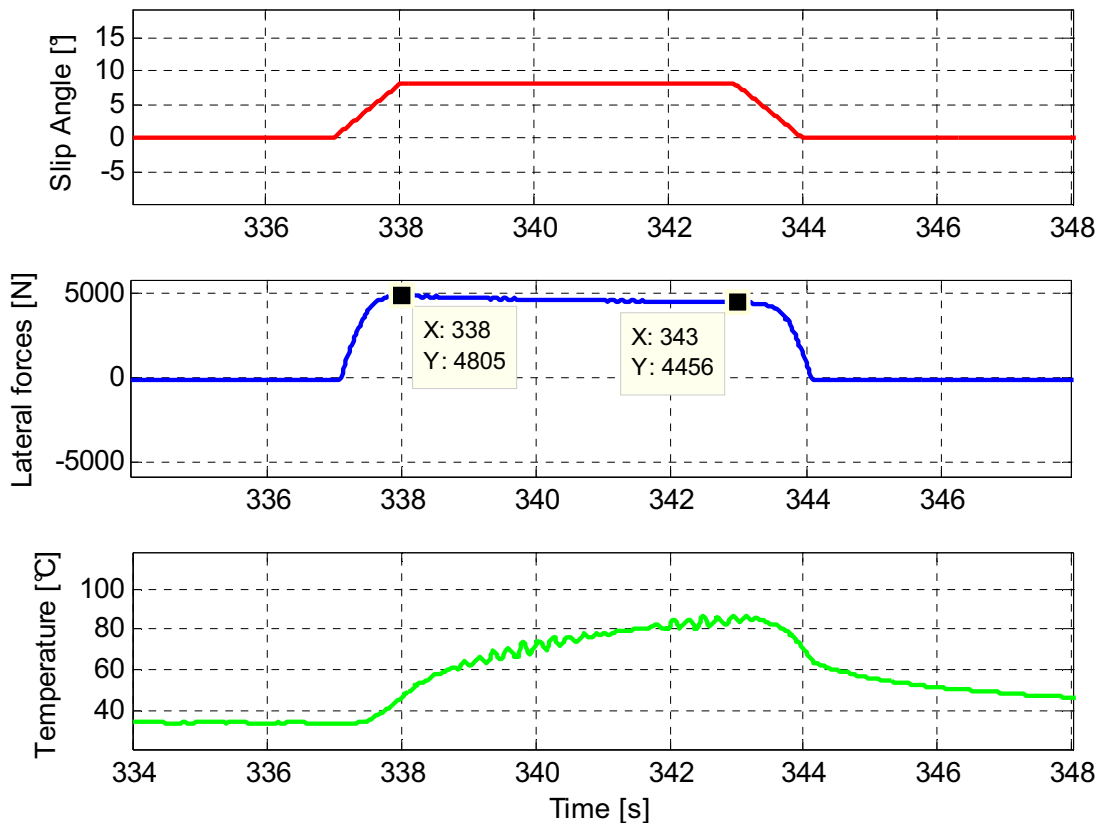


Figure 20: Lateral force and temperature results at 110 km/h

In these graphs, the interesting area to look at is the time period where the slip angle is constant from 338 to 343 seconds. A non negligible decrease of lateral force of about 350N can be seen when the tire is heating up. Its temperature goes from 46 to 86°C so the decrease of lateral force is around 8.75N/°C for a constant slip angle, which is very close to what has been observed in the earlier work [6].

The lateral force and the tire cornering stiffness as functions of the temperature within the five second period where the slip angle is constant (same case as previously) are plotted on the following graphs.

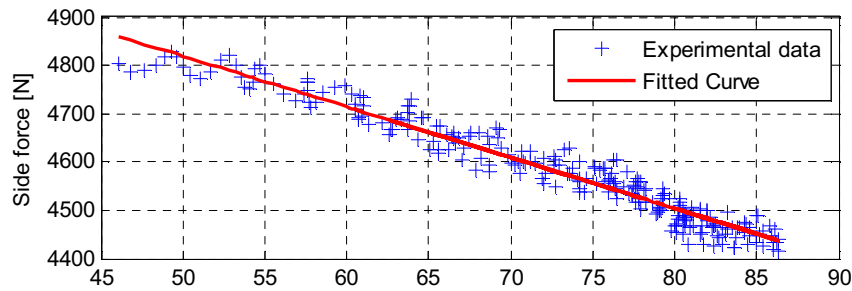


Figure 21: Lateral force variation as function of temperature

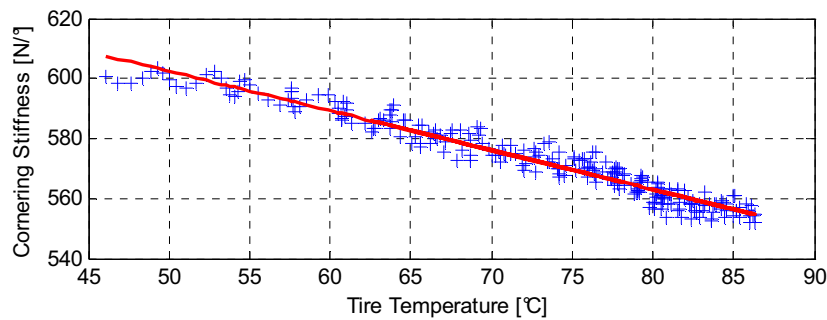


Figure 22: Cornering stiffness variation as function of the temperature

As highlighted by the red fitted curves, both parameter variations are linear. Even if this is not shown here, the same conclusion can be drawn for all tested slip angle values (from 2 to 18°). The tables below sum up the slopes found in each tested condition for the lateral force and the cornering stiffness.

Table 3: Slopes of  $F_y$  (Temperature)

	Slip angle [°] →	2	5	8	-8	12	18
Slope [N/°C]	50 km/h	-4,4	-2,6	-14,4	-11,3	-10,3	-11,7
	110 km/h	-6,2	-10,1	-8,8	-8,3	-8,0	-6,9

Table 4: Slopes of cornering stiffness (Temperature)

	Slip angle [°] →	2	5	8	-8	12	18
Slope [N/°C]	50 km/h	-2,2	-2,0	-1,8	-1,4	-0,9	-0,7
	110 km/h	-2,7	-2,0	-1,3	-1,0	-0,7	-0,4

As it can be seen from these tables, the decrease of transmissible lateral force is not constant and varies depending on conditions. There is unfortunately no obvious tendency that could allow an understanding on how the temperature makes the friction

coefficient to decrease. Regarding the cornering stiffness, a conclusion can be drawn. Actually, an increase in temperature for a small slip angle (linear domain) implies an important reduction in tire cornering stiffness. However, in the non linear domain, the decrease in cornering stiffness is lower when the temperature increases. With less certainty, one could also observe that for a high vehicle speed, the derivative of the cornering stiffness in function of the temperature decreases faster than for low speed. This means that in the linear domain, the cornering stiffness reduction will be greater at high speed but in the non linear domain, it will be lower. These conclusions along with the fact that both parameters decrease linearly with the temperature will allow developing a thermal effects model based on the currently used Pacejka magic formula and taking into account the variation in lateral force due to the tire tread temperature.

## 5 Tire thermal model development

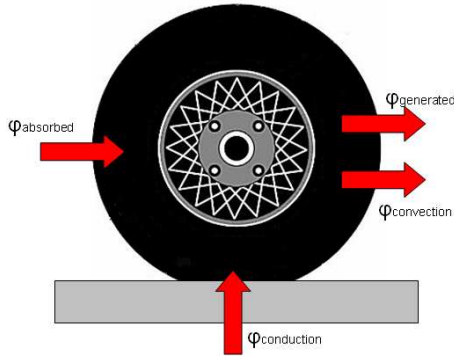
As seen in Fig.1, the thermal effects model can be implemented in the Delft-Tyre model by developing a temperature model and a thermal effects model. The temperature model estimates the tire tread temperature as function of the inputs defined previously in Fig.14. The thermal effects model estimates the variation in lateral force due to the temperature and is implemented in series with the temperature model.

### 5.1 Tire tread temperature model

Two different approaches have been used in order to develop the tire tread temperature model. The first approach was to build a model completely physical based on a power heat balance between the tire and its surrounding environment. However, it will be seen that this approach did not provide satisfying results. Therefore, a second approach was to build an empirical model based on tire inputs with sensitivity coefficients to be determined experimentally.

#### 5.1.1 Physical temperature model

The first approach was to derive a physical model based on a power heat balance between the tire tread surface and its surrounding environment. The studied tire can be represented by the scheme below and the heat balance can be written as follows.



$$\begin{aligned}
 \varphi_{conv} + \varphi_{abs} &= \varphi_{cond} + \varphi_{gen} \\
 \varphi_{conv} &= h \times (A_{total} - A_{cp}) \times (T - T_a) \\
 \varphi_{cond} &= -\lambda \times A_{cp} \times \frac{\partial T}{\partial x} \\
 \varphi_{absorbed} &= \rho \times V \times c \times \frac{\partial T}{\partial t} \\
 \varphi_{generated} &= \dot{q} \times V
 \end{aligned} \tag{5.1}$$

Figure 23: Scheme of the studied tire (heat balance)

Assuming that the road surface temperature is at ambient temperature, the heat balance equation to be solved can be written as below with  $\rho$  the air density,  $V$  the volume,  $c$  the specific heat capacity,  $h$  the heat transfer coefficient,  $A_{cp}$  the contact patch area,  $V$  the vehicle speed,  $\lambda$  the thermal conductivity,  $q$  the heat flux and  $T_a$  the air temperature.

$$\rho \times V \times c \times \frac{\partial T}{\partial t} - h \times (A_{total} - A_{cp}) \times (T - T_a) = \dot{q} \times V - \lambda \times A_{cp} \times (T - T_a) \tag{5.2}$$

Then, by assuming that the generated heat flux is entirely due to the friction between the tire and the road, one can write:

$$\dot{q} \times V = F_y \times \omega \times R \times \alpha \quad (5.3)$$

with  $\omega$  the rotational wheel speed and R the effective wheel radius.

Hence, the final equation can be written as follows:

$$W \times \frac{\partial T}{\partial t} - h \times (A_{total} - A_{cp}) \times (T - T_a) = F_y \times \omega \times R \times \alpha - \lambda \times A_{cp} \times (T - T_a) \quad (5.4)$$

This is a first order linear differential equation. Therefore, its solution is an exponential function of time which is not ideal especially for long simulations. As expected, this solution depends on the slip angle and the vehicle speed, the two most influent input parameters seen in the sensitivity study.

$$T(t) = \frac{-K_3}{K_2} + (T_{initial} + \frac{K_3}{K_2}) \times e^{\frac{K_2}{K_1} \times t} \quad (5.5)$$

$$K_1 = W \quad (5.6)$$

$$K_2 = h \times (A_{total} - A_{cp}) - \lambda \times A_{cp}$$

$$K_3 = F_y \times \omega \times R \times \alpha - T_a \times K_2$$

where the unknown parameters W (heat capacity), h (convection coefficient) and  $\lambda$  (heat conductivity) are to be determined experimentally and the estimated temperature can be plotted to be compared with Flat-Trac measurement data.

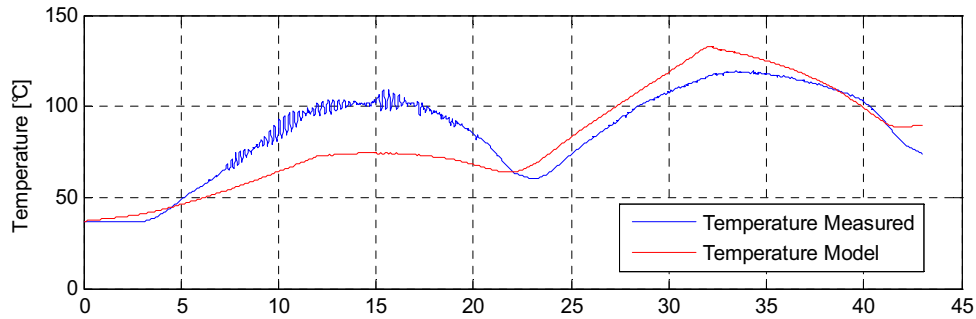


Figure 24: Example of physical temperature model result

However, once the unknown coefficients identified, the result is not satisfying as it can be seen on the graph above. The model accuracy is not acceptable and it gets even worse for a long time simulation. Because of this conclusion, another approach has been used and will be explained in the following part.

## 5.1.2 Empirical temperature model

The second approach was to derive an empirical temperature model based on input parameters (slip and camber angles, vehicle speed, pressure and normal load). Basically, the tire temperature can be estimated in real time by a quadratic function represented by the formula below.



$$T(t = n) = C_k T(t = n - 1) + \sum_{i=1}^5 C_k P_i^2 + \sum_{i=1}^5 C_k P_i + \sum_{i=1}^5 \sum_{j=2}^5 C_k P_i P_j + C_k$$

with  $C_k$  some constant unknown coefficients to be determined experimentally during indoor experiments on the Flat-Trac bench and  $P_i$  input parameters.

### 5.1.3 Coefficients optimization

In this tire tread temperature model, around twenty unknown coefficients are to be determined experimentally. The cost function  $f$  to be optimized as close to zero as possible was:

$$f = \frac{\sqrt{\sum (T_{model} - T_{ref})^2}}{\sqrt{\sum T_{ref}^2}} \times 100 \quad (5.7)$$

It is important to determine unknown coefficients on test profile including as many solicitations a tire can go through as possible. In this way, the model should be accurate enough for different types of operating conditions and therefore more robust. For this reason, the test profile consists of different types of solicitations.

Once the coefficients are optimized, the estimated temperature can be plotted to be compared with the measured temperature.

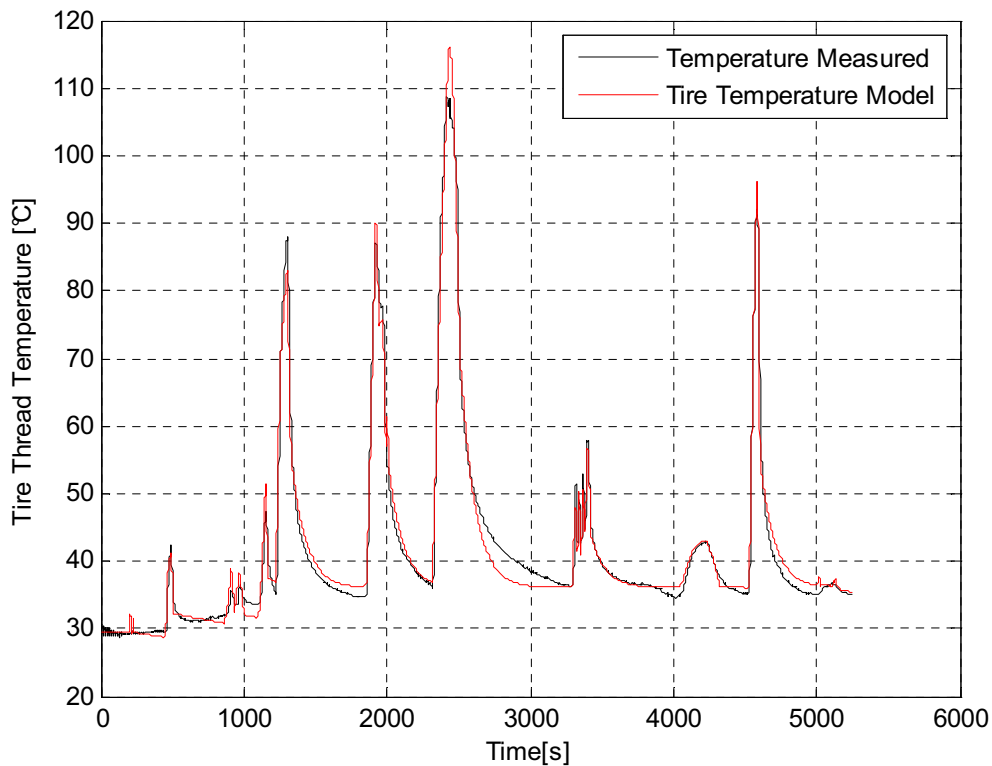
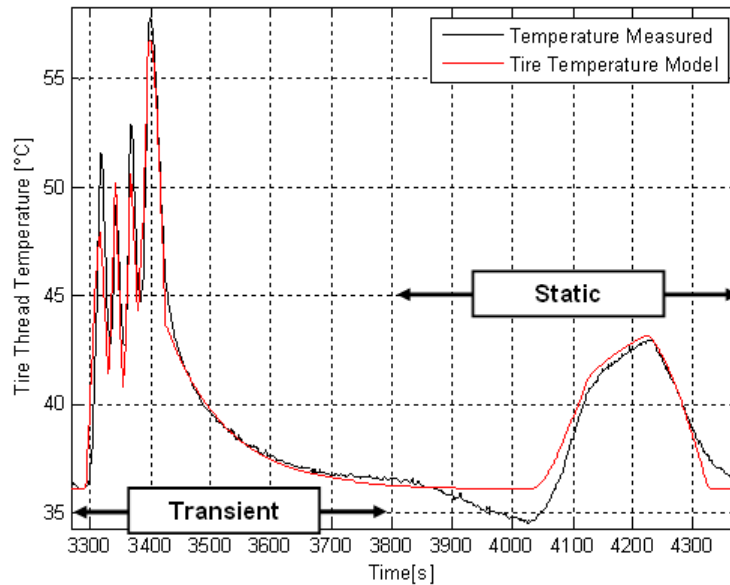


Figure 25: Tire temperature model results

As it can be seen, the tire temperature model accuracy is very satisfying. The instantaneous error never goes up to 10°C (less than 20% for the relative error) and the mean error is equal to 1.39°C on this profile. As explained earlier, the model has to be accurate in static and transient conditions. Fig.26 shows a zoom in on the graph above where these two conditions occur. It can be seen that the tire tread temperature model behaves very well in both conditions.



**Figure 26: Temperature model results (Zoom in static and transient conditions)**

Furthermore, as seen earlier, the tire tread temperature increases strongly and makes the lateral forces decrease in the non linear domain. Therefore, it is of paramount importance to estimate the temperature accurately for large slip angles. Fig.28 shows that the temperature is well estimated for different slip angle profiles and values.

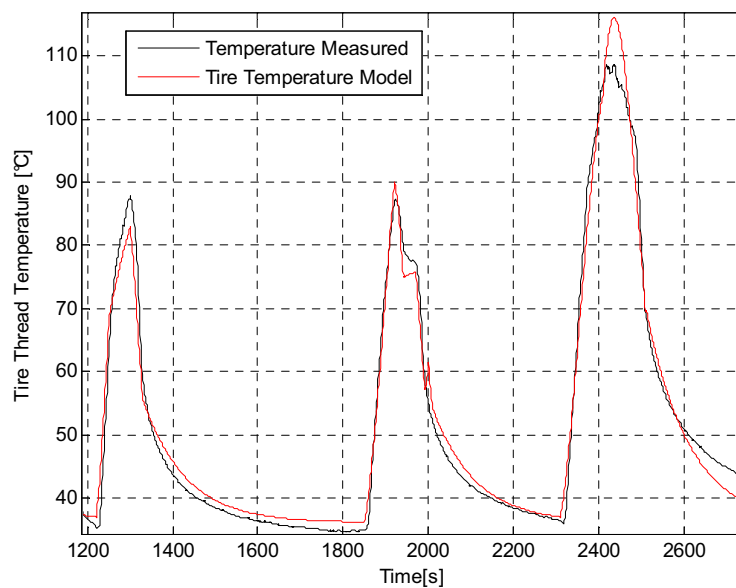


**Figure 27: Temperature model results (zoom in non linear region)**

As a conclusion to this part, one can say that this tire tread temperature model is accurate enough to be used as the input temperature  $T$  of the thermal effect model estimating the variation of lateral force due to the tire temperature. This thermal effects model is depicted in the next part.

## 5.2 Lateral force model with thermal effect

As seen in part 4.3, in the transversal direction, two different tire parameters vary linearly with the tire tread temperature. These parameters are the maximum lateral force and the tire cornering stiffness. In the Pacejka magic formula, these two parameters are respectively represented by the coefficients  $D_y$  and  $K_y$ . These coefficients are constant and determined experimentally using a standard procedure.

### 5.2.1 Model construction

From the conclusions drawn previously and from the literature, the decrease of lateral force is linearly dependent on the tire temperature  $T$ . Therefore, it can be taken into account by making the coefficients  $D_y$  and  $K_y$  decreasing with the temperature as below.

$$\begin{aligned} D_y(T) &= f(D_{y0}, \frac{\partial \mu}{\partial T}, T, T_m) \\ K_y(T) &= f(K_{y0}, \frac{\partial C_p}{\partial T}, T, T_m) \end{aligned} \tag{5.8}$$

$$B_y(T) = \frac{K_y(T)}{C_y \times D_y(T)}$$

Where:

- $D_{y0}$  and  $K_{y0}$  are the peak constant values of the tire lateral force model and the cornering stiffness (in steady state without thermal effects)
- $\frac{\partial \mu}{\partial T}$  is the change in maximum lateral force that the tire can transmit to the road with the tire surface temperature
- $\frac{\partial C_p}{\partial T}$  is the change in cornering stiffness with tire surface temperature
- $T_m$  is a reference temperature

The two derivative unknown parameters are to be determined experimentally and correspond to the slopes described in part 4.3 when performing constant sideslip stages. As seen previously, values for those parameters are not constants and depend on the vehicle speed and the slip angle. This is partly a reference temperature  $T_m$  has been added. Actually, this temperature is a function of the vehicle speed and the slip angle. In that way, Pacejka's coefficients are function of the variation of temperature a tire goes through.

After including the new coefficients function of the temperature, the Magic Formula for the lateral force becomes:

$$F_y(\alpha, T) = D_y(T) \times \sin^{-1}(C_y \tan^{-1}(B_y(T) \times \alpha - E_y(B_y(T) \times \alpha - \tan^{-1}(B_y(T) \times \alpha)))) + S_{vy}$$

$$\alpha = \alpha^* + S_{hy}$$

The following step is to optimize the unknown parameters so that the difference between the measured lateral forces and the estimated lateral forces will be as small as possible.

## 5.2.2 Coefficients optimization

In the thermal effects model, only two unknown parameters are to be determined experimentally. A standard test procedure from Renault [2][3] has been used to optimize these two parameters. This procedure is generally used to characterize a tire in pure transversal direction and in steady-state condition. Using this procedure, transient phenomena were avoided and only the thermal phenomena were taken into account by the optimization. The cost function  $f$  representing the temperature error to be optimized as close to zero as possible was:

$$f = \frac{\sqrt{\sum (Fy_{model} - Fy_{ref})^2}}{\sqrt{\sum Fy_{ref}^2}} \times 100 \quad (5.9)$$

Once these two parameters are optimized, the following graphs have been obtained (Figs. 29, 30 and 31). The currently used Pacejka model without thermal effects is represented by the black curve, the Pacejka model with thermal effects by the red curve and the measured lateral force by the blue curve. To get an idea of the solicitation the tire went through during this test, the green curve shows the slip angle (times 100). This test is a slip angle sweep from  $-18^\circ$  to  $18^\circ$  keeping all other input parameters constant. In such a case, the tire temperature climbs very quickly as it can be seen in the following graph.

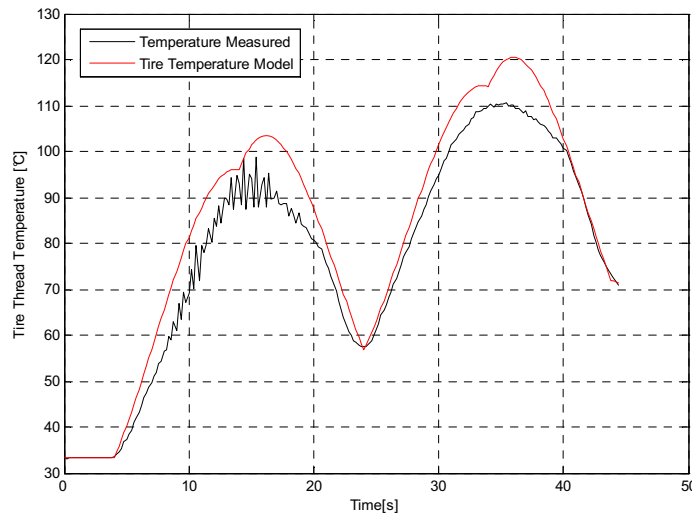
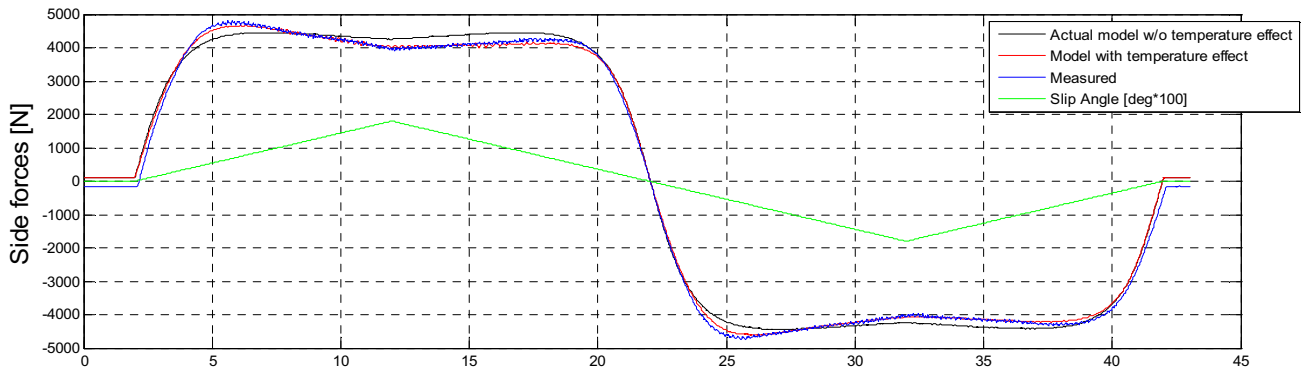


Figure 28: Tire temperature for a SA sweep

In the first lateral force graph, the consideration by the thermal effect model of the lateral force decrease due to an increase in temperature is clearly visible. The basic magic formula seems to take the average for a slip angle solicitation and underestimate the lateral force in the sideslip increasing phase and overestimate it in the descending phase.



**Figure 29: Comparison models for SA sweep ( $F_y$  vs time)**

The following graph illustrates the instantaneous error between the measured lateral force and the two models (with and without thermal effects). It can be seen that the accuracy of the model which takes into account the tire temperature is better than the basic Pacejka magic formula. Actually, the mean error is about two times less for this test (98N with thermal effect against 194N for Pacejka).

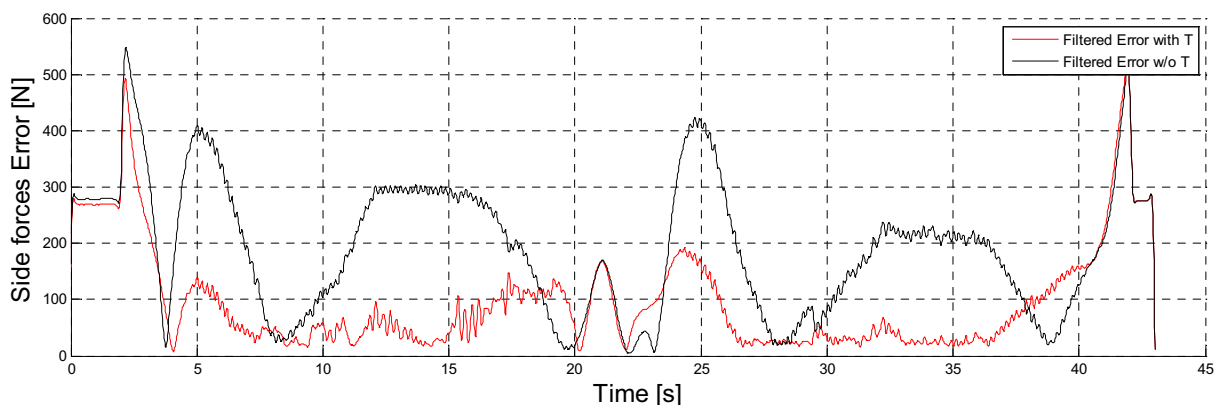


**Figure 30: Comparison models for SA sweep (Instantaneous errors)**

Fig. 31 still illustrates the measured and modeled lateral forces during the same test but in function of the slip angle. This allows identifying the loss in lateral force a tire can produce due to an increase in tread temperature during the descending phase.

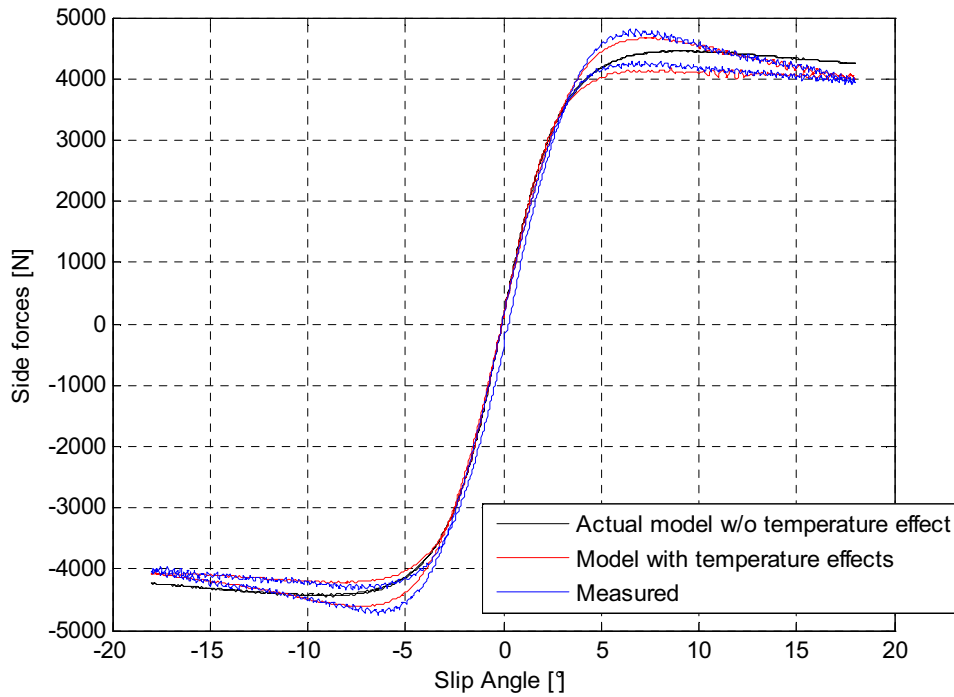


**Figure 31: Comparison models for SA sweep ( $F_y$  vs SA)**

To conclude with these graphs, one can say that the precision of the model with thermal effects is better than the basic Pacejka magic formula, in particularly in the non linear domain (greater than  $\pm 4^\circ$ ). The decrease in lateral force due to the tire temperature is taken into account very well.

Regarding the linear domain, the mean temperature  $T_m$  is almost the same as the instantaneous temperature  $T$ . Therefore, the model with thermal effects behaves as the Pacejka model since the difference of these two temperature values is almost zero.



## 6 Extension of the model to vehicle use

In order to extend the thermal effects model validity to vehicle use, full vehicle tests on Renault tracks have been performed. The vehicle and its equipment have been depicted in the materials part.

The main difference between these vehicle tests and the tests performed on the Flat-Trac bench is mainly the tire surrounding environment. Actually, in road conditions, aerodynamics phenomena due to the vehicle speed occur. Hence, the tire tread is cooled by convection. This phenomenon does not occur when performing Flat-Trac experiments because the tire has no translational speed. Moreover, some thermal effects due to the dissipated heat from the engine can heat the ambient air in the wheelhouse. On the Flat-Trac bench, the surrounding air is controlled and kept constant.

Therefore, these two phenomena could modify the tire tread temperature and the temperature model does not take them into account as it has been developed on the Flat-Trac bench. In other words, the model may not be accurate enough for vehicle use. Thus, the objective of this part is to quantify how important the surrounding environment influence is on the tire temperature and a way to go from the Flat-Trac model to a vehicle model will be described.

### 6.1 Ambient temperature and aerodynamics influences

In order to study the ambient temperature influence on the tire tread temperature and to find a relationship between the wheelhouse air and tire tread temperatures, a static test (vehicle at rest) have been performed with the thermal engine running. The engine temperature increasing progressively, the wheelhouse air temperature increases as well. Test results are illustrated on the following graph. The black curve represents the engine temperature, the blue one the wheelhouse air (ambient) temperature and the red one the tire tread temperature.

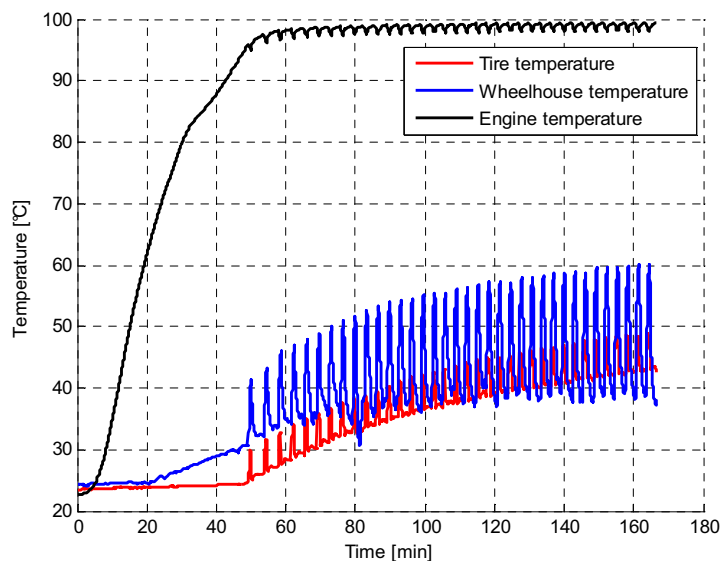
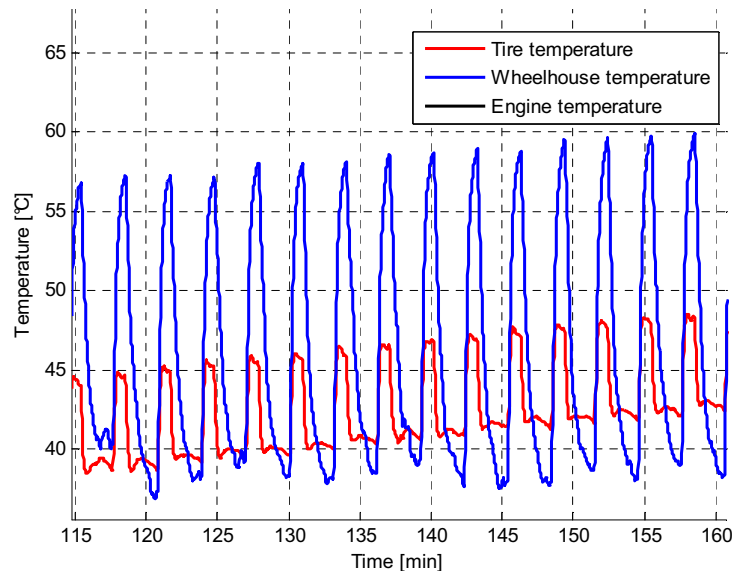


Figure 32: Ambient temperature influence (static test)



As it can be observed, the ambient temperature increases along with the engine temperature. This ambient temperature makes also the tire tread temperature increase slowly. From about 50 minutes of test, one can observe temperature variations due to the cooling system ventilator switching on and off. This latter moves the hot air coming from the engine to the wheelhouses. Therefore, the ambient air temperature increases and decreases quickly. The following picture is a zoom in in Fig. 32 and illustrates this phenomenon.



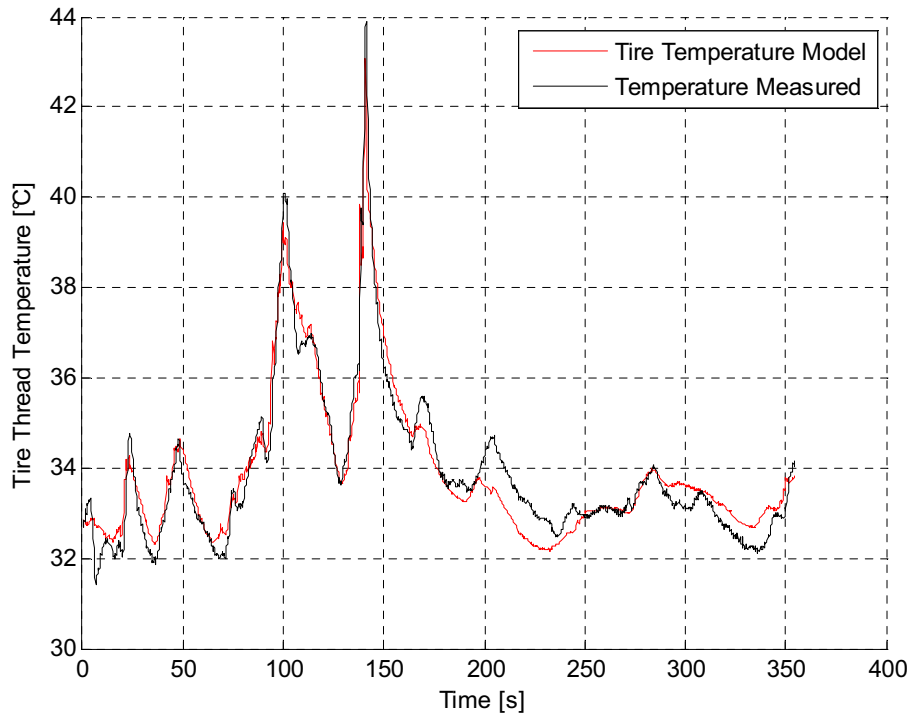
*Figure 33: Zoom in static test*

Fig. 33 shows that an increase of the ambient temperature makes the tire tread temperature increase instantaneously. On the contrary, a decrease of the ambient temperature makes the tire tread temperature decrease instantaneously. It can be concluded that the ambient temperature influence is important and that the tire tread temperature model used on tracks should take into account this parameter.

Regarding the tire cooling by forced convection due to aerodynamics effects, it can be taken into account by modifying the sensitivity coefficient values for the vehicle speed. Actually, this cooling is only function of the vehicle speed. During the thermal analysis on the Flat-Trac bench, the vehicle speed influence was non negligible and positive. An increase in speed resulted in an increase in tire tread temperature. On vehicle, an increase in speed makes the tire temperature decrease due to an increase in cooling by convection. The vehicle speed influence becomes therefore negative.

## 6.2 Temperature modeling

As described in the previous part, the tire tread temperature model developed on the Flat-Trac bench can be adapted to full vehicle use by taking into account the ambient temperature in the wheelhouse and by modifying the sensitivity coefficient values for the speed. These coefficients have been optimized on two laps of the behavior track at the Renault test facility. Measured and estimated temperatures are represented in the Fig. 34.



**Figure 34: Temperature model on tracks (Optimization)**

The relative error between both temperatures on this test profile is 1.26% (0.37°C for the absolute error), which is very satisfying. In order to validate this model and check its precision and its robustness, a test on the constant radius area ( $R = 50$  meters) has been performed at high speed (around 65 km/h) to obtain a slip angle of around  $6^\circ$ . The measured and estimated temperatures are illustrated below.

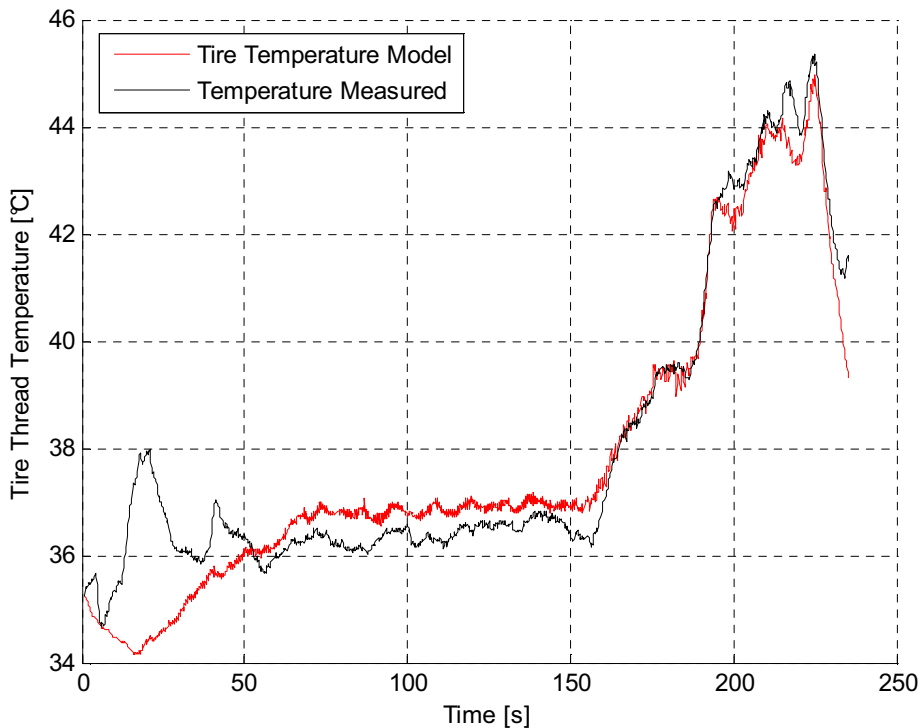


**Figure 35: Temperature model on tracks (Validation)**

The tire tread temperature model precision is satisfying on this profile as well. In fact, the relative error is 1.32% (0.59°C for the absolute error). Therefore, this model can be used when using the thermal effects model on tracks.

In terms of lateral force variation, the modeling principle remains identical. The two thermal coefficients estimating the derivatives of the friction  $\mu$  and the tire cornering stiffness are optimized for the track model. Unfortunately, one can observe that the tire temperature on two laps of behavior track does not increase enough to have an important effect on the lateral force, except between 130 and 150 seconds where the temperature reaches 44°C (see Fig. 34).

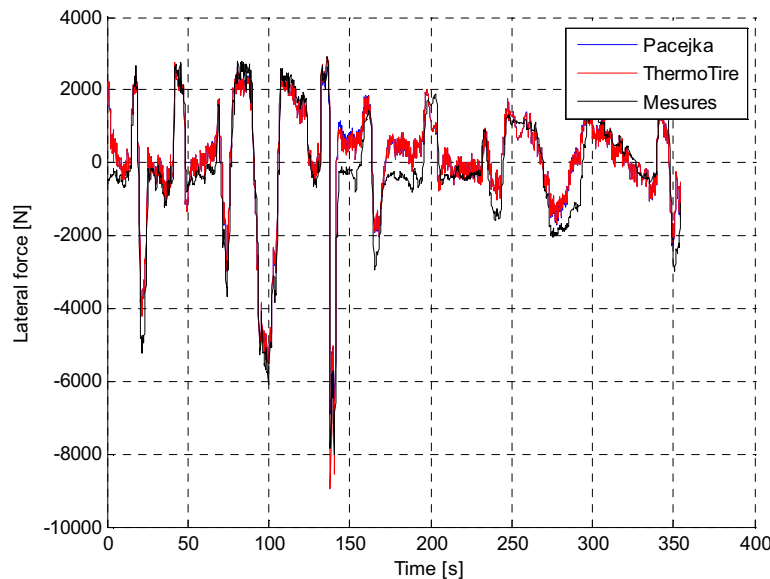


**Figure 36: Lateral force model (2 laps of behavior track), ThermoTire is the name for the Pacejka model with thermal effects**

The following graph is a zoom in on Fig. 36 for the time interval 125 to 170 seconds.

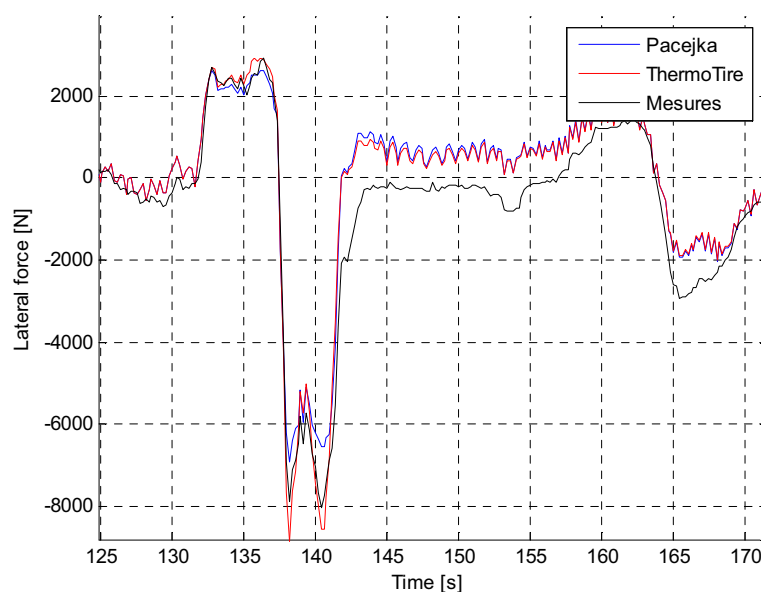


**Figure 37: Zoom in of lateral force model (2 laps of behavior track)**

It can be seen that when the tire temperature is high enough, the thermal effects model allows having a better precision for the lateral force. Actually, the mean absolute errors on these 2 laps are 494.7N for the actual model and 491.5N for the thermal effects model. These 3 Newtons are 'gained' only in the time interval where the temperature increases between 130 and 150 seconds.

### **6.3 Conclusion**

The tire tread temperature can be modeled by using the same method that is used on the Flat-Trac bench. However, it is necessary to take into account the wheelhouse air temperature and to modify the sensitivity coefficient values relative to the vehicle speed.

The lateral force variations can be modeled as on the Flat-Trac bench without any modifications. The thermal effects model allows improving the model precision when a change in tire temperature occurs. Nevertheless, it has been seen that it would be necessary to perform some more constraining and longer tests in order the tire temperature to have a more important effect on the lateral force.



## 7 Conclusion

In order to attain the objectives, several steps were needed to go through. Actually, at the beginning of this study, a thermal analysis of a tire has been performed on a Flat-Trac bench. It has allowed getting an understanding on the tire temperature influence. In fact, it has been seen that the correlation between the tire tread temperature and its performance in terms of forces is significant.

The tire tread temperature is mainly influenced by the sideslip angle. Actually, the relative motion between part of the tire tread and the road surface implies important friction phenomena increasing the tire temperature.

An increase of temperature introduces a non negligible decrease of transmissible forces for given operating conditions. This decrease occurs mainly in the non linear regions (slip angle up to around  $4^\circ$  in transversal direction) and is due to a linear decrease of two parameters in function of the tire temperature, the friction coefficient  $\mu$  and the tire cornering stiffness.

The experiments results have led to a thermal effects model that can be implemented in parallel to the Pacejka magic formula (see Fig.1). This thermal effects model consists of two sub-models. The first model estimates the tire tread temperature in function of the operating conditions and the second estimates the lateral force decrease occurring due to the temperature increase. These two models are implemented in series together and in parallel to the Pacejka magic formula to estimate the lateral force (see Fig.1). In the linear region (down to  $4^\circ$  of slip angle), the thermal effects model is not so useful because the temperature does not increase much. The temperature is less influent on tire forces and its effect can be neglected. In that case, the thermal effects model behaves almost exactly like the “basic” magic formula.

In order to extend the thermal effects model validity to a vehicle use, a set of full-vehicle experiments has been performed. Some differences have to be taken into account. Actually, on the Flat-Trac bench, the ambient temperature is controlled and constant which is not the case in on-road conditions. Moreover, the aerodynamic effects are different since the wheel on the Flat-Trac bench has no longitudinal speed. Therefore, these on-road tests allow the tire surrounding air temperature influence as well as aerodynamics effects to be quantified. Finally, the thermal effects model has been modified to be used in real tire operating conditions.

As a future work, further more constraining and longer tests should be done because the thermal effects are less due to aerodynamic effects. Then, the thermal effects model could be extended in the longitudinal direction when experimental materials allow it. Then, a study could be performed in order to model the transient behaviour of the tire. Nowadays, the Pacejka magic formula is accurate only in steady-state conditions.



## Appendices

### Appendix A: Delft-Tyre model details in x and y directions

#### *Steady-state longitudinal direction (pure slip)*

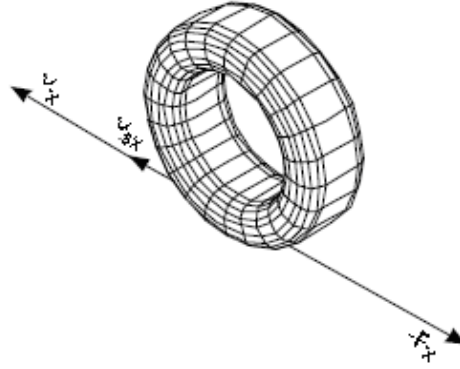


**Figure 38: Pure braking/traction condition from [10]**

$$F_x = F_{x0}(S_x, F_z)$$

$$F_{x0} = D_x \sin \left[ C_x \tan^{-1} \left\{ B_x S_x - E_x (B_x S_x - \tan^{-1}(B_x S_x)) \right\} \right] + S_{Vx}$$

$$S_x = S_x + S_{Hx}$$

$$M_y = (S_{Vx} + K_x S_{Hx}) R_0$$

With:

$$C_x = P_{Cx1} \cdot \lambda_{Cx}$$

$$D_x = \mu_x \cdot F_z$$

$$\mu_x = (P_{Dx1} + P_{Dx2} \cdot df_z) \cdot \lambda_{\mu x}$$

$$E_x = (P_{Ex1} + P_{Ex2} \cdot df_z + P_{Ex3} \cdot df_z^2) \{1 - P_{Ex4} \cdot \text{sgn}(S_x)\} \cdot \lambda_{Ex}$$

$$K_x = F_z \cdot (P_{Kx1} + P_{Kx2} \cdot df_z) \cdot \exp(P_{Kx3} \cdot df_z) \cdot \lambda_{Kx}$$

$$B_x = K_x / (C_x D_x)$$

$$S_{Hx} = (P_{Hx1} + P_{Hx2} \cdot df_z) \cdot \lambda_{Hx}$$

$$S_{Vx} = F_z (P_{Vx1} + P_{Vx2} \cdot df_z) \cdot \lambda_{Vx} \cdot \lambda_{\mu x}$$

With:

---

$P_{Cx1}$	Shape factor C
$P_{Dx1}, P_{Dx2}$	Peak factor D
$P_{Ex1}, P_{Ex2}, P_{Ex3}, P_{Ex4}$	Curvature factor E
$P_{Kx1}, P_{Kx2}, P_{Kx3}$	Slip stiffness BCD
$P_{Hx1}, P_{Hx2}$	Horizontal shift H
$P_{Vx1}, P_{Vx2}$	Vertical shift V

---



## Steady-state lateral direction (pure sideslip)

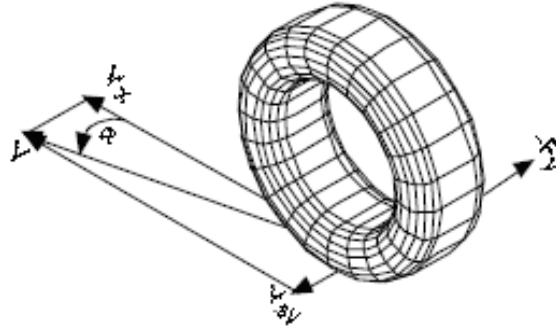


**Figure 39: Pure cornering condition**

$$F_y = F_{y0}(\alpha, \gamma, F_Z)$$

$$F_{y0} = D_y \sin[C_y \tan^{-1}\{B_y \alpha_y - E_y (B_y \alpha_y - \tan^{-1}(B_y \alpha_y))\}] + S_{Vy}$$

$$\alpha_y = \alpha + S_{Hy}$$

$$\gamma_y = \gamma \cdot \lambda_{\gamma}$$

With:

$$C_y = P_{Cy1} \cdot \lambda_{Cy}$$

$$D_y = \mu_y \cdot F_Z$$

$$\mu_y = (P_{Dy1} + P_{Dy2} \cdot df_z) (1 - P_{Dy3} \cdot \gamma_y^2) \lambda_{\mu y}$$

$$E_y = (P_{Ey1} + P_{Ey2} \cdot df_z) \cdot \{1 - (P_{Ey3} + P_{Ey4} \cdot \gamma_y) \operatorname{sgn}(\alpha_y)\} \lambda_{Ey}$$

$$K_y = P_{Ky1} \cdot F_{Z0} \cdot \sin[2 \cdot \tan^{-1}\{F_Z / (P_{Ky2} \cdot F_{Z0} \cdot \lambda_{Fz0})\}] (1 - P_{Ky3} |\gamma_y|) \lambda_{Fz0} \cdot \lambda_{Ky}$$

$$B_y = K_y / (C_y D_y)$$

$$S_{Hy} = (P_{Hy1} + P_{Hy2} \cdot df_z + P_{Hy3} \cdot \gamma_y) \cdot \lambda_{Hy}$$

$$S_{Vy} = F_Z (P_{Vy1} + P_{Vy2} \cdot df_z + (P_{Vy3} + P_{Vy4} \cdot df_z) \gamma_y) \lambda_{Vy} \cdot \lambda_{\mu y}$$

With:

---

$P_{Cy1}$	Shape factor C
$P_{Dy1}, P_{Dy2}, P_{Dy3}$	Peak factor D
$P_{Ey1}, P_{Ey2}, P_{Ey3}, P_{Ey4}$	Curvature factor E
$P_{Ky1}, P_{Ky2}, P_{Ky3}$	Slip stiffness BCD
$P_{Hy1}, P_{Hy2}, P_{Hy3}$	Horizontal shift H
$P_{Vy1}, P_{Vy2}, P_{Vy3}, P_{Vy4}$	Vertical shift V

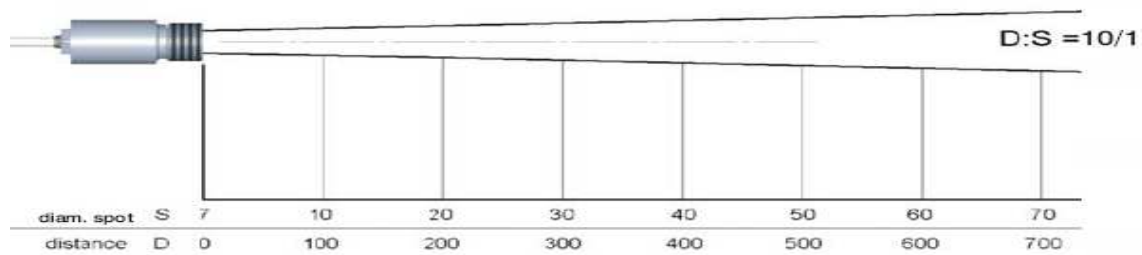
---

## Appendix B: Infrared temperature sensors specifications

Measurement specifications	
Model	CS-SF10-C1
Optical resolution	10:1
Temperature range <sup>1</sup>	-20 to 350°C
Spectral range	8 to 14μm
System accuracy <sup>2</sup>	±1.5% or ±1.5°C
Repeatability <sup>2</sup>	±0.75% or ±0.75°C
Temperature resolution <sup>3</sup>	0.2°C
Response time	30ms to 999s (90%), adjustable
Emissivity/gain	0.100 to 1.100 (adjustable via 0 to 5V DC input or software)
Transmissivity/gain <sup>1</sup>	0.100 to 1.100
Signal processing <sup>1</sup>	peak hold, valley hold, average
Certificate of calibration	optional
Electrical specifications	
Outputs/analog	0 to 5V or 0 to 10V 1/10/100 mV/ °C
Outputs/digital	optional USB or Alarm
Inputs	programmable functional input for external emissivity/ambient temperature adjustment (0 to 5VDC), hold function or RS232 / USB (optional) communication
Cable length	1m (standard), 3m, 8m, 15m
Power supply	15mA (5 to 7VDC), 9mA (12 to 28VDC)
General specifications	
Environmental rating	IP 65 (NEMA-4)
Ambient temperature	-20°C to 75°C
Storage temperature	-20°C to 85°C
Relative humidity	10 to 95%, non condensing
Vibration	IEC 68-2-6: 3 G, 11 to 200Hz, any axis
Shock	IEC 68-2-27: 50 G, 11ms, any axis
Weight	58g

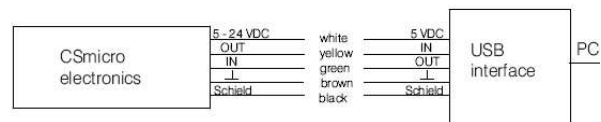
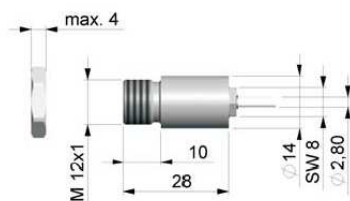
<sup>1</sup> adjustable via software  
<sup>2</sup> ambient temperature: 23 ±5°C, whichever is greater, object temperature ≥0°C  
<sup>3</sup> temperature of the object <100°C and time constant >0.2s

### Spécifications optiques



### CS avec optique standard SF

#### Dimensions/ Raccordements



## Appendix C: Test matrix from the experimental design

Test	Average	1 SA $\alpha$	2 CA $\gamma$	3 Normal load Fz	4 Speed V	5 Pressure P	I. 1/2 $\alpha/\gamma$	I. 1/3 $\alpha/Fz$	I. 1/4 S/ $\alpha$	I. 1/5 $\alpha/P$	I. 2/3 Fz/ $\gamma$	I. 2/4 S/ $\gamma$	I. 2/5 $\gamma/P$	I. 3/4 S/Fz	I. 3/5 Fz/P	I. 4/5 S/P
1	+	-	-	-	-	-	+	+	+	+	+	+	+	+	+	+
2	+	+	-	-	-	-	-	-	-	-	+	+	+	+	+	+
3	+	-	+	-	-	-	+	+	+	+	-	-	-	+	+	+
4	+	+	+	-	-	-	+	-	-	-	-	-	-	+	+	+
5	+	-	+	+	-	-	+	+	+	+	-	+	+	-	-	+
6	+	+	-	+	-	-	-	-	-	-	-	+	+	-	-	+
7	+	-	+	+	-	-	+	+	+	+	+	-	-	-	-	+
8	+	+	+	+	-	-	+	-	-	-	+	-	-	-	-	+
9	+	-	-	-	+	-	+	+	+	+	+	-	+	-	+	-
10	+	+	-	-	+	-	-	+	-	-	+	+	+	+	+	-
11	+	-	+	-	+	-	-	-	+	+	-	-	-	-	+	-
12	+	+	+	-	+	-	+	+	-	-	-	+	-	-	+	-
13	+	-	+	+	+	-	-	-	+	+	-	-	+	+	-	-
14	+	+	-	+	+	-	-	+	-	-	-	+	+	-	-	-
15	+	-	+	+	+	-	-	-	+	+	+	+	-	-	-	-
16	+	+	+	+	+	-	+	+	-	-	+	+	-	+	-	-
17	+	-	-	-	-	+	+	+	+	+	+	+	-	+	-	-
18	+	+	-	-	+	+	-	-	-	-	+	+	-	-	-	-
19	+	-	+	-	-	+	+	+	-	-	-	-	+	+	-	-
20	+	+	+	-	-	+	+	-	+	+	-	-	+	+	-	-
21	+	-	+	+	-	+	+	+	-	-	-	+	-	-	+	-
22	+	+	-	+	-	+	-	-	+	+	+	+	-	+	+	-
23	+	-	+	+	-	+	-	+	-	-	+	-	+	+	-	-
24	+	+	+	+	-	+	+	-	+	+	+	-	+	+	-	-
25	+	-	-	-	+	+	+	-	-	-	+	-	-	-	-	+
26	+	+	-	-	+	+	-	+	-	-	+	-	-	-	-	+
27	+	-	+	-	+	+	-	-	-	-	-	+	+	-	-	+
28	+	+	+	-	+	+	+	+	+	+	-	+	+	-	-	+
29	+	-	-	+	+	+	+	-	-	-	-	-	-	+	+	+
30	+	+	-	+	+	+	-	+	+	+	-	-	-	+	+	+
31	+	-	+	+	+	+	-	-	-	-	+	+	+	+	+	+
32	+	+	+	+	+	+	+	+	+	+	+	+	+	+	+	+

Table legend:

- + signs represent high level value of input parameters or interactions
- - signs represent low level value of input parameters or interactions
- I. = interaction between two input parameters

The 32 cases are divided into 8 principal tests during which the normal load, the vehicle speed and the inflation pressure are kept constant. Only the slip and camber angles vary as illustrated by the following graph. The slip angle is represented by the blue curve and the camber angle by the red one.

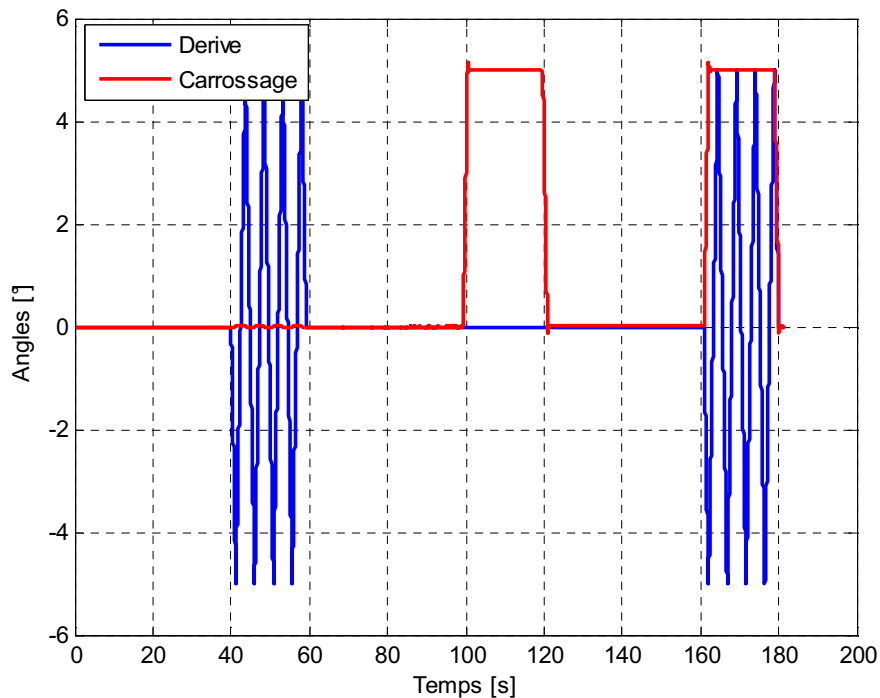


**Figure 40: Slip and camber angles from the experimental design**

According to the conclusion from previous projects [2], the tire temperature can be ‘reinitialized’ tending to a value between 30 and 35°C depending on previous solicitations the tire went through. To reach this value, the tire needs to roll in straight line for some time without any change in input parameters. Therefore, between each 32 cases, the tire rolls in straight line for 40 seconds without slip or camber angle and with no input parameter variation.

To date, the table below sums up the different levels taken by the input parameters.

**Table 5: Values taken by input parameters from experimental design**

	Low level -	High level +	Unit
<b>Slip angle <math>\alpha</math></b>	0	-/+ 5	°
<b>Camber angle <math>\gamma</math></b>	0	5	°
<b>Normal load <math>F_z</math></b>	2500	6000	N
<b>Speed <math>V</math></b>	30	110	km/h
<b>Pressure <math>P</math></b>	1.8	3.4	Bar



## References

- [1] Sorniotti A. (2009): '*Tire Thermal Model for Enhanced Vehicle Dynamics Simulation*'. SAE international publication 2009-01-0441.
- [2] Comte J., Faurie JM. (2009): '*Setting of a tire surface temperature measuring system on Flat-Trac*' (Translation from French title 'Mise en place du moyen de mesure de la température des pneumatiques sur FT'). Renault SA technical note n°68261-2009-0441, Aubevoye, 2009.
- [3] Comte J., Faurie JM. (2009): '*Benchmarking on tire temperature measuring systems*' (Translation from French title 'Bibliographie sur les mesures de la température appliquées aux pneumatiques'). Renault SA technical note n°68261-2009-0440, Aubevoye, 2009.
- [4] Février P., Martin H., Fandard G. (2008): '*Method for simulating the thermo-mechanical behaviour of a tyre rolling on the ground*'. Patent from Michelin. {March} 2008, international ref. number: WO 2008/025892 A1.
- [5] Février P. (2008): '*Thermal and Mechanical Tire Force & Moment Model presentation*'. 4<sup>th</sup> Intelligent Tire Technology Automotive Conference, Wiesbaden October 2003.
- [6] Kraus A., Netsch L., Berkmüller M., Schick B. (2006): '*T3M – Tüv Tire Temperature Method presentation*'. TÜV Automotive GmbH. *Tire Technology Expo 2006*, Stuttgart, March 2006.
- [7] Smith N. (2004): '*Understanding Parameters Influencing Tire Modeling*'. Colorado State University, 2004 Formula SAE Platform.
- [8] Masahiko M. (2003): '*Development of Tire Side Force Model Based on "Magic Formula" with the Influence of Tire Surface Temperature*'. R&D Review of Toyota CRDL, Vol. 38, No. 4, October 2003.
- [9] Société de Technologie Michelin (2001): '*Tire grip mechanisms*' (Translation from French title 'Les mécanismes de l'adhérence sur routes'). Pages 8 to 54.
- [10] TNO (1996), '*MF-Tyre User Manual Version 5.0*'. Pages 15 to 30.
- [11] Dufournier Technologies website  
[http://dufournier.technologies.perso.neuf.fr/francais/fr\\_produits\\_modele\\_pneu.htm](http://dufournier.technologies.perso.neuf.fr/francais/fr_produits_modele_pneu.htm)
- [12] Renault SA intranet: <http://declic.intra.renault.fr./wps/portal>
- [13] Lamy C., Basset M., Romieu P. (2008): '*Estimation of tire slip angle and wheel motion by combination of inertial and GPS measurements using an extended Kalman filter*', Mulhouse, 2008.

[14] <http://www.micro-epsilon.com/company/group/Optris.html>

[15] Texense website: <http://www.texense.com/?lang=fr>